



Review

# The Influence of Alloying Elements on the Microstructure and Properties of Al-Si-Based Casting Alloys: A Review

Bruna Callegari <sup>1</sup>, Tiago Nunes Lima <sup>1</sup> and Rodrigo Santiago Coelho <sup>1,2,\*</sup>

<sup>1</sup> SENAI CIMATEC, Instituto SENAI de Inovação em Conformação e União de Materiais (CIMATEC ISI C&UM), Av. Orlando Gomes 1845, Salvador 41650-010, Brazil; bruna.callegari@fieb.org.br (B.C.); tiago.nunes@fieb.org.br (T.N.L.)

<sup>2</sup> Centro Universitário SENAI CIMATEC, Programa de Pós-Graduação GETEC/MPDS/MCTI, Av. Orlando Gomes, 1845, Salvador 41650-010, Brazil

\* Correspondence: rodrigo.coelho@fieb.org.br

**Abstract:** The excellent casting behavior and mechanical and corrosion properties of aluminum-silicon (Al-Si)-based alloys make them ideal for the manufacture of lightweight components with complex geometries. However, these properties depend directly on their microstructure, which, in its turn, is strongly affected by the composition of the alloy, among other factors. Several elements can be added to the material aiming to promote microstructural changes, e.g., grain refinement, optimization of phase morphology and distribution, and precipitation strengthening. Efforts are continuously put into such enhancements of cast Al alloys since they lead to quality improvements that allow for weight reduction and safety increase. Considering the technological relevance of the subject, this paper provides an overview of the research focused on the addition of alloying elements to these alloys, with a greater focus on Al-Si-based systems and the comprehension of the effects of these additions on their microstructure and properties.

**Keywords:** aluminum alloys; casting; chemical composition; microstructure; properties



**Citation:** Callegari, B.; Lima, T.N.; Coelho, R.S. The Influence of Alloying Elements on the Microstructure and Properties of Al-Si-Based Casting Alloys: A Review. *Metals* **2023**, *13*, 1174. <https://doi.org/10.3390/met13071174>

Academic Editor: Amogelang Bolokang

Received: 31 May 2023

Revised: 19 June 2023

Accepted: 22 June 2023

Published: 24 June 2023



**Copyright:** © 2023 by the authors. Licensee MDPI, Basel, Switzerland. This article is an open access article distributed under the terms and conditions of the Creative Commons Attribution (CC BY) license (<https://creativecommons.org/licenses/by/4.0/>).

## 1. Introduction

Aluminum (Al) alloys are employed in various industrial segments that rely on their reduced weight combined with good mechanical, corrosion, thermal and electrical properties. Despite their relatively low strength, their strength-to-weight ratio is superior to those of most metals [1]. Aluminum is one of the most versatile metals for casting, being extensively used in the automotive industry due to its extremely valuable weight-saving potential. As of 2015, there were more than 300 casting aluminum alloys registered at The Aluminum Association (Arlington, VA, USA). Its advantages for casting include its low melting point, negligible gas solubility (except for hydrogen) and good surface finishing of cast products. On the other hand, some alloy classes present considerable solidification shrinkage. Also, high dispersion of mechanical properties is observed, and these properties are usually lower than those obtained in wrought alloys [2].

Silicon (Si)-containing alloys are the most relevant for casting, especially to the enhanced fluidity provided by high amounts of the eutectic Al-Si phase and by silicon's enthalpy of fusion (1810 kJ/kg, against 395 kJ/kg for aluminum), that increases the time during which the melted alloy can flow through a mold before becoming too cold. Other advantages of the Al-Si system are its good weldability, corrosion resistance and low solidification shrinkage levels [2]. The addition of magnesium (Mg) to the system establishes the basis for a family of alloys that combine excellent casting properties with great mechanical properties after heat treatment, in addition to elevated corrosion resistance and low thermal expansion. Although not as resistant as copper (Cu)-containing alloys, Al-Si-Mg ones present relatively good mechanical properties [3]. A great share of sand- or permanent-mold cast parts are from A356 (Al—7% Si—0.3% Mg, or simply Al-7Si-0.3Mg) or A357

(Al—7% Si—0.5% Mg, or simply Al-7Si-0.5Mg) alloys [2]. These alloys are widely used in the fabrication of automotive components, which, though not as strong as forged ones, are preferred due to higher design versatility, dimensional accuracy and still acceptable strength levels. Casting alloys for the automotive industry must, in general, present low hot tearing and shrinkage susceptibility, and high impact, fatigue and corrosion resistance [4].

To define properties, several elements can be added to aluminum alloys. These additions may act according to various mechanisms upon the microstructures and properties of alloys. Main mechanisms for improvement of cast alloys include microstructural refinement, both in terms of dendritic arm spacing and of dendritic grains; modification of the morphology of eutectic phases, leading to refinement, globularization and homogeneous distribution; modification or neutralization of iron (Fe)-rich intermetallics, provided that Fe is the most critical impurity in cast Al alloys, promoting phases with the embrittling character when combined with Al and Si; and promotion of precipitates, including during aging treatment, that can increase hardness, strength and thermal stability. In these alloys, elements can be categorized into three groups, although one should bear in mind that, at times, a single element can perform more than one role [3,5]:

- Main/basic elements are added in higher amounts and mainly control castability and the evolution of properties;
- Secondary/doping elements in lower amounts provide support for effects such as solidification behavior control, microstructural refinement and modification of phase morphology, promotion or suppression of secondary phase formation and reduction of oxidation.
- Impurities, being elements whose control is limited due to the fabrication process, can affect castability and form insoluble phases that may either limit or, at times, improve certain properties.

The comprehension of the effects of different additions to Al castings is of vital importance to the design and improvement of alloys. Such developments can lead to several positive outcomes, such as superior performance of components and reduction of weight and energy consumption. Features most extensively reviewed in the literature are the effects of iron (e.g., [6]) and strontium (e.g., [7]) on the quality and microstructure of Al-Si-based alloys. More recent reviews provide relatively summarized discussions about the effects of alloying elements due to the assessment of additional aspects, such as particle reinforcements [8] and processing conditions [9]. Campbell developed a brief review covering several points ranging from nucleation and growth of eutectics and oxides to texture development and hydrogen embrittlement in Al alloys [10]. However, no work has been carried out in-depth to compile and discuss the effects of alloying additions according to the main effects they can impart on these alloys.

In this context, the purpose of this review is to provide a critical assessment of the effect of additions to casting aluminum alloys, with a focus on, but not limited to, hypoeutectic Al-Si-based alloys. Such an effect is mainly characterized in terms of microstructural evolution correlated with mechanical properties and, to a lesser extent, corrosion behavior. It encompasses a wide range of elements, which were divided into six categories, as illustrated in Figure 1, primarily defined according to the main purposes of their addition to alloys. These involve main elements, eutectic morphology modifiers, grain refiners, and iron and modifiers of the  $\beta$ -AlFeSi. One section was dedicated to rare earth elements, and a sixth section comprised other transition elements added with general purposes, such as dispersoid precipitation to enhance high-temperature properties. All alloy compositions are provided in weight percent unless otherwise stated, even when the percent symbol is omitted for simplification.

Legend:

- Main elements (grey)
- Eutectic modifiers (yellow)
- Grain refiners (cyan)
- beta-AlFeSi neutralizers (purple)
- Rare earths (blue)
- Others (green)

1 IA 1A H Hydrogen 1.008	2 IIA 2A He Helium 4.003																	18 VIIIA 8A									
3 Li Lithium 6.941	4 Be Beryllium 9.012																	5 B Boron 10.811	6 C Carbon 12.011	7 N Nitrogen 14.007	8 O Oxygen 15.999	9 F Fluorine 18.998	10 Ne Neon 20.180				
11 Na Sodium 22.990	12 Mg Magnesium 24.305	13 Al Aluminum 26.982	14 Si Silicon 28.086	15 P Phosphorus 30.974	16 S Sulfur 32.066	17 Cl Chlorine 35.453	18 Ar Argon 39.948											29 Cu Copper 63.546	30 Zn Zinc 65.38	31 Ga Gallium 69.723	32 Ge Germanium 72.631	33 As Arsenic 74.922	34 Se Selenium 78.971	35 Br Bromine 79.904	36 Kr Krypton 83.798		
19 K Potassium 39.098	20 Ca Calcium 40.078	21 Sc Scandium 44.956	22 Ti Titanium 47.867	23 V Vanadium 50.942	24 Cr Chromium 51.996	25 Mn Manganese 54.938	26 Fe Iron 55.845	27 Co Cobalt 58.933	28 Ni Nickel 58.693	29 Cu Copper 63.546	30 Zn Zinc 65.38	31 Ga Gallium 69.723	32 Ge Germanium 72.631	33 As Arsenic 74.922	34 Se Selenium 78.971	35 Br Bromine 79.904	36 Kr Krypton 83.798										
37 Rb Rubidium 85.468	38 Sr Strontium 87.62	39 Y Yttrium 88.906	40 Zr Zirconium 91.224	41 Nb Niobium 92.906	42 Mo Molybdenum 95.95	43 Tc Technetium 98.907	44 Ru Ruthenium 101.07	45 Rh Rhodium 102.906	46 Pd Palladium 106.42	47 Ag Silver 107.868	48 Cd Cadmium 112.414	49 In Indium 114.818	50 Sn Tin 118.711	51 Sb Antimony 121.760	52 Te Tellurium 127.6	53 I Iodine 126.904	54 Xe Xenon 131.294										
55 Cs Cesium 132.905	56 Ba Barium 137.328	57-71 Lanthanide Series	72 Hf Hafnium 178.49	73 Ta Tantalum 180.948	74 W Tungsten 183.84	75 Re Rhenium 186.207	76 Os Osmium 190.23	77 Ir Iridium 192.217	78 Pt Platinum 195.085	79 Au Gold 196.967	80 Hg Mercury 200.592	81 Tl Thallium 204.383	82 Pb Lead 207.2	83 Bi Bismuth 208.980	84 Po Polonium [208.982]	85 At Astatine 209.987	86 Rn Radon 222.018										
87 Fr Francium 223.020	88 Ra Radium 226.025	89-103 Actinide Series	104 Rf Rutherfordium [261]	105 Db Dubnium [262]	106 Sg Seaborgium [266]	107 Bh Bohrium [264]	108 Hs Hassium [269]	109 Mt Meitnerium [278]	110 Ds Darmstadtium [281]	111 Rg Roentgenium [280]	112 Cn Copernicium [285]	113 Nh Nihonium [286]	114 Fl Flerovium [289]	115 Mc Moscovium [289]	116 Lv Livermorium [293]	117 Ts Tennessine [294]	118 Og Oganesson [294]										
			57 La Lanthanum 138.905	58 Ce Cerium 140.116	59 Pr Praseodymium 140.908	60 Nd Neodymium 144.245	61 Pm Promethium 144.913	62 Sm Samarium 150.36	63 Eu Europium 151.964	64 Gd Gadolinium 157.25	65 Tb Terbium 158.925	66 Dy Dysprosium 162.500	67 Ho Holmium 164.930	68 Er Erbium 167.259	69 Tm Thulium 168.934	70 Yb Ytterbium 173.055	71 Lu Lutetium 174.967										
			89 Ac Actinium 227.028	90 Th Thorium 232.038	91 Pa Protactinium 231.036	92 U Uranium 238.029	93 Np Neptunium 237.048	94 Pu Plutonium 244.064	95 Am Americium 243.061	96 Cm Curium 247.070	97 Bk Berkelium 247.070	98 Cf Californium 251.080	99 Es Einsteinium [254]	100 Fm Fermium 257.095	101 Md Mendelevium 258.1	102 No Nobelium 259.101	103 Lr Lawrencium [262]										

Figure 1. Representative periodic table with indication of the main elements covered in this review, classified into specific groups according to different colors.

## 2. Effects of Alloying Elements

### 2.1. Main Elements

As aforementioned, silicon is the main addition to cast aluminum alloys due to its positive effect on fluidity. Abdel-Jaber et al. verified a continuous increase in strength upon the increase of Si concentration from 3% to 15% in Al, while ductility was enhanced only up to the eutectic composition (ca. 12%) [11]. In as-cast Al-Si-0.4Mg alloys containing 0.12–0.13% Ti modified with 100–150 ppm Sr, the continuous increase of Si content from 6.55% to 14.43% led to a clear strength increase up to an amount of 11.4%; for higher amounts, a higher spread of results was seen. However, a clear trend of ductility decrease with the increase of Si content within the entire assessed range was also observed [12]. In cast and hot-extruded Al-Si-0.5Mg alloys containing up to 0.15% Fe, increasing Si content from 0.58% to 7% and 12.3% led to a continuous strength increase, both in as-cast and extruded conditions [13]. In Al-Si-Cu-Mg alloys, the presence of higher silicon amounts (9% vs. 4.5%) was acknowledged as responsible for refining Fe-rich intermetallics, which will be discussed ahead (see Section 2.4), as well as dispersing clusters of both Fe- and Cu-rich intermetallic particles to interdendritic and intergranular regions. Such modification is beneficial to restrain crack propagation, leading to improved ductility [14]. The positive effect of increasing Si content from 1.5% to 6% in a 7075-T6 alloy on strength has also been reported [15].

Regarding corrosion, Si is present as a secondary phase embedded in the matrix [1]. The electrochemical behavior of dispersed particles differs from that of the matrix, meaning they might act as anodes or cathodes with respect to the matrix, leading to the formation of galvanic pairs [16,17]. Si is cathodic and is present in relatively high amounts in cast Al alloys [1]. Thus, one may expect that galvanic corrosion takes place, especially in refined structures, with a higher degree of dispersion of the eutectic phase within dendrites and with a higher contact area between Si particles and the matrix, which has been observed in some studies, e.g., [18–20]. Nevertheless, in practice, the effect of Si on overall corrosion resistance can be regarded as negligible due to the low current density and the fact that

Si particles are highly polarized [1]. In fact, Öztürk et al. verified that the modification of eutectic morphology by strontium (Sr) addition (see Section 2.2) in reasonable amounts could actually contribute to improving the corrosion resistance of the A356 alloy. After permanent mold casting, the optimum amount of Sr in this sense was 120 ppm, and after sand mold casting, it was 170 ppm [21]. The corrosion resistance of 3xx alloys is much more impacted by the presence of impurities as iron (Fe) and copper (Cu), that form insoluble and relatively coarse intermetallics [16].

Kaba et al. evaluated the suitability for automotive applications of alloys with lower Si content, namely 5%, as opposed to the typical content of about 7%, under the assumption that lower concentrations of the element could contribute positively to grain refinement because the element has a poisoning effect over the action of Ti-B-based refiners (see Section 2.3). However, comparing alloys containing 5% and 7% Si with the same amounts of Mg (0.3%), Ti (0.1%), Sr (200 ppm) and Al-5Ti-1B refiner (0.01%), they verified that the alloy with lower Si content, despite presenting finer grains due to the reduction of the poisoning effect, presented higher interdendritic spacing ( $76.7 \pm 11.0 \mu\text{m}$  vs.  $53.5 \pm 8.0 \mu\text{m}$ ), caused by the lower amount of eutectic phase, yielding reduced strength and ductility, as opposed to what was expected [4]. This shows that dendrite refinement is more decisive to mechanical properties than grain refinement. Furthermore, the reduced fluidity of alloys leaner in Si suggests that such reduction is not favorable to castability.

On the other hand, Abalymov et al. assessed the suitability of alloys with higher silicon content, motivated by the fact that the casting of hypoeutectic alloys can be accompanied by certain issues because their fluidity is lower than that of eutectic ones. Thus, to cast geometrically complex components, it may be necessary to overheat the melt and certain regions of the mold, which can lead to microstructural heterogeneities and increased porosity. The filling capacity of the mold can be enhanced using properly designed feeders, which not only increases metal consumption but also might still be insufficient to overcome these limitations, depending on the size of the part and level of complexity. Therefore, the use of eutectic systems can eliminate some casting limitations. In their work, the addition of 0.25% Mg to an Al-11.2Si alloy provided sufficient hardenability upon T6 treatment to allow the achievement of mechanical properties as adequate as those of the currently used alloy and equally compliant with requirements for certain automotive applications. However, attention must be paid to the significant drop in ductility for higher Mg additions [22].

The amount of Si also affects porosity distribution. In Al-Cu-based alloys, it was shown that the addition of the element reduces hydrogen solubility in the liquid Al phase, leading to shorter times for micro-pore nucleation and, consequently, larger final porosity [23]. With respect to the combined effects of Si (0, 1% and 9%) and Sr (200 ppm), which is commonly used to modify the eutectic morphology, it was observed that the addition of Sr caused a porosity increase in pure Al and in the Al-1Si alloy, and decrease in the Al-9Si alloy. In all cases, however, Sr addition led to the reduction of pore size and average area, and the smallest values was found in the 1% Si alloy, both with and without Sr. When it comes to pore distribution, no noticeable effect was seen in pure Al and in the 1% Si alloy; in 9% Si, however, the addition of Sr affected distribution significantly, as schematically shown in Figure 2. The model proposed to explain pore distribution states that, in pure Al, solidification takes place from the walls to the center of the mold, resulting in on main shrinkage defect after solidification, whereas in the 1% Si alloy, the low fraction of eutectic phase within dendrites leads to the formation of small voids by the accumulation of small volumes of liquid metal on the solidification front. Because the amount of eutectic is null or too low in these cases, the addition of Sr does not have any significant effect. In the 9% Si alloy, however, the absence of modification causes preferential eutectic nucleation on dendrite boundaries, growing from walls to center, resulting in a concentration of porosity in the center, where the last interdendritic regions become solid; upon Sr addition, eutectic nucleation takes place independently from dendrites, causing porosity to distribute more homogeneously [24].

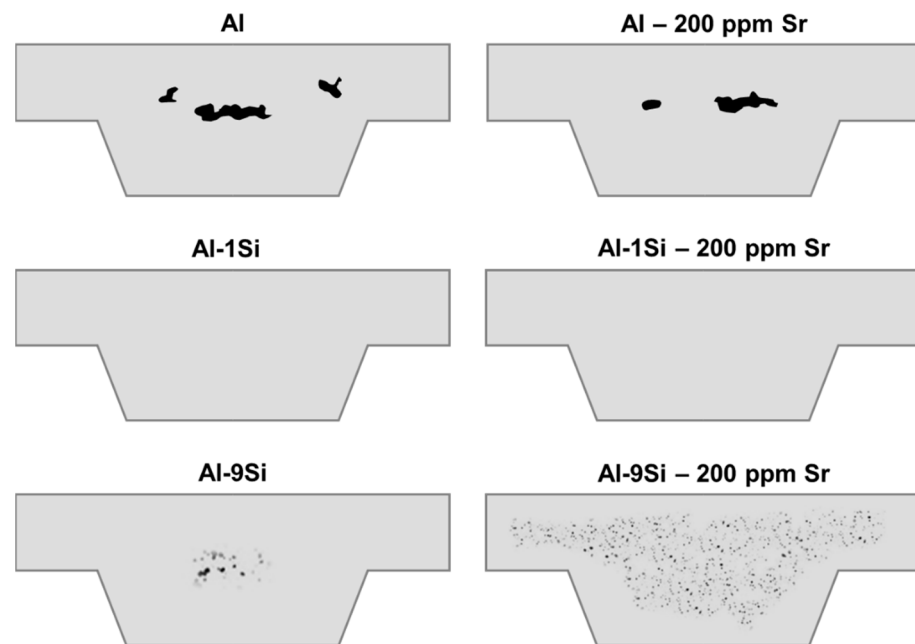


**Figure 2.** Influence of Si content and Sr addition on porosity distribution in Al alloys (data from [24]).

As for Mg, it is the main responsible, along with Cu, for the hardening of cast Al alloys upon heat treatment. Higher amounts of the element can increase the degree of precipitation hardening but, on the other hand, promote the formation of the so-called  $\pi$ -AlFeMgSi phase ( $\text{Al}_5\text{Si}_6\text{Mg}_5\text{Fe}_2$ ), a Fe-rich intermetallic that may cause embrittlement of the alloy [2]. Regardless, the conversion of the needle-like  $\beta$ -AlFeSi phase, which will be discussed ahead, into the Chinese script  $\pi$ -AlFeMgSi with the increase of Mg content in the presence of Fe reduces the deleterious effects of the prior on mechanical properties [25]. The decomposition of the  $\pi$  phase during solution treatment is vital not only to reduce embrittling effects but also to increase the amounts of Si and Mg in solution for later age hardening purposes [26]. Furui et al. showed that, although not as effective in increasing isothermal peak hardness, increasing the amount of Mg from 0.5% to 0.8% in an Al-10Si alloy considerably reduces the aging time needed to achieve such hardness [27].

In the A356 alloy, the increase of magnesium content results in higher yield strength and strain hardening rate [16]. Yielding behavior and the quality index ( $Q = UTS + 150\log(A)$ , where  $UTS$  is the ultimate tensile stress and  $A$  is the percent elongation to fracture [28]) present an apparently parabolic dependence with the amount of Mg in the range between 0.3 and 0.7%. The quality index evolution can be explained by the fact that, although ultimate strength increases, ductility is severely limited by the addition of Mg, and the quality index represents a balance between strength and elongation [29]. Still, in A356, the same parabolic-like tendency for the quality index was observed as a function of Mg content (0.25–0.39%) by different authors [30].

Increasing Mg concentration from 0.5 to 2.7% in an Al-7.6Si alloy has been shown to promote dendritic refinement [31]. On the other hand, Huang, Liu and Li concluded that the addition of 0.4% Mg to an Al-7Si alloy appears to partially hinder the effects of Sr and Na as modifiers of eutectic morphology (see Section 2.2), which was explained in the grounds that Mg addition results in the formation of Mg-rich phases in the final stages of solidification, affecting modification of the associated eutectic phase forming simultaneously [32].

As stated above, the addition of copper can increase the alloy's strength due to precipitation hardening effects upon heat treatment. The addition of Cu to Al-7Si-Mg alloys [33], including A356 [34,35], and the combined addition of Cu (3–5%) and Fe (0.3–0.8%) to Al-13Si alloys [36] led to strength improvement, while the simultaneous addition of Cu (0.09–2.76%) and Mn (0.01–0.43%) to Al-Si-Mg alloys resulted in microstructural refinement and increase

of fatigue strength at high temperatures [37]. In an Al-7Si-0.4Mg alloy, Cu additions up to 3% altered the fatigue crack propagation pathway from trans-dendritic to inter-dendritic due to the precipitation of Cu-rich intermetallics that behave as obstacles to propagation within the matrix [38]. In high-pressure-die-cast (HPDC) Al-9Si-Cu alloys with different Mg additions, the amounts of Cu and Mg are suggested to act together upon mechanical strength evolution: in alloys containing up to 0.3% Mg, properties were enhanced up to a Cu amount of 4.9%, whereas such enhancement took place for Cu concentrations up to 3.6% in alloys containing 0.1% Mg. This difference was attributed to the lowering of solvus lines in alloys with higher Mg content, increasing solid solubility of these elements. Furthermore, alloys with higher Mg and Cu contents also presented faster responses to aging treatments [39]. In a thixocast Al-7Si-0.5Mg, the addition of Cu up to 0.5% was effective to increase strength after a T5 temper (direct aging after casting) without any significant loss in ductility. However, higher additions—1.0%—hinder elongation properties, and even higher ones—1.5%—lead to strength reduction as well. Property improvement with additions up to 0.5% Cu was attributed to the precipitation of non-shearable  $\theta'$  particles that contributed more effectively to hardening than the Mg-based  $\beta''$  phase. In lower fractions and uniform distribution,  $\theta'$  phase brings positive contributions; in excess, on the other hand, it imparts an embrittling effect on the alloy [40]. Furthermore, increasing Cu concentration in Al-Si-Mg alloys can also lead to porosity increase [41].

## 2.2. Modifiers of the Eutectic Morphology

The eutectic phase is composed of the solid solution of Al and pure Si, with an approximate composition of Al—12.6% Si, and forms at about 577.6 °C (Figure 3). Most commercial alloys are hypoeutectic, i.e., possess Si contents lower than the eutectic one but still contain the eutectic phase in their microstructure. This phase can present extremely coarse morphologies, especially under low cooling rates, consisting of Si plates or needles embedded in the matrix. The presence of these morphologies results in limited ductility due to their embrittling nature. Faster cooling can help overcome this issue due to refinement effects. However, the morphology of the eutectic phase can also be modified by the action of certain elements [2]. The addition of calcium (Ca), sodium (Na), strontium (Sr) and antimony (Sb), among others, can modify the eutectic morphology, producing a finer, fibrous structure. Such modification takes place by the suppression of crystal growth or by the balance between matrix and Si growth rates. The result is a considerable improvement in mechanical properties, especially ductility [3]. The biggest benefits of eutectic modification are obtained in alloys containing from 5% Si up to the eutectic composition, but these benefits depend on the degree to which the porosity related to the addition of modifiers can be overcome or restricted [3].

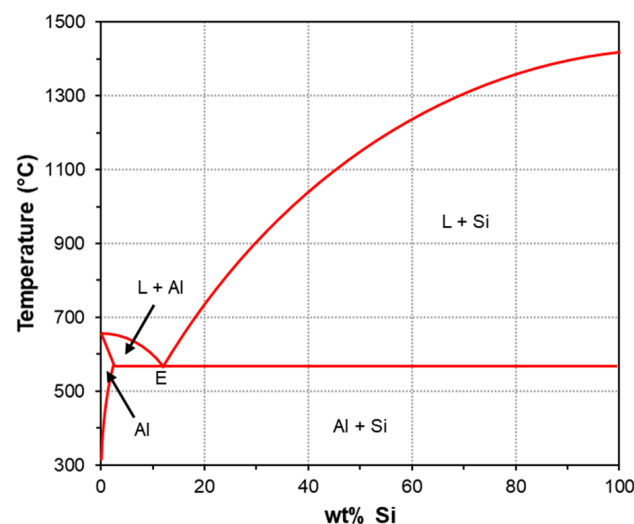
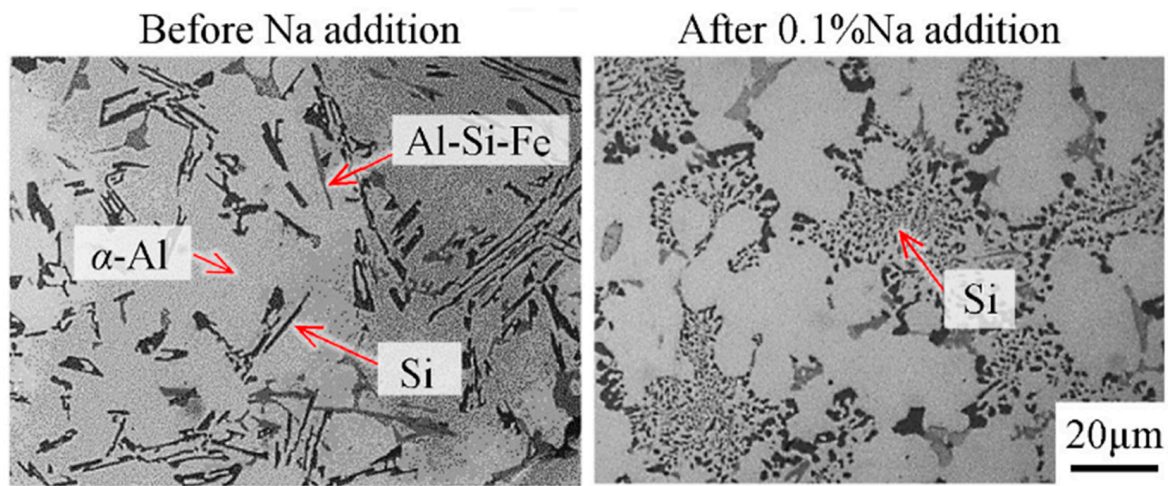


Figure 3. Al-Si phase diagram (E: eutectic point).

For many years, the modification in Al-Si systems was accomplished by the addition of small amounts (50–150 ppm) of Na in metallic or salt form to the melt. Sodium reduces the eutectic temperature by approximately 12 °C, reducing the nucleation capacity of the eutectic phase. A possible explanation for its action lies in the neutralization of the effect of phosphorus impurities that act as nucleation sites for coarse particles by the formation of NaP. On the other hand, sodium in excess may lead to the formation of the AlNaSi phase, which limits its modifying action. During growth, it is believed that Na limits the phenomenon by accumulating on the surface of particles. Yet another theory suggests the effect of twinning in Si crystals, forcing them to grow in different crystallographic directions, originating the fibrous aspect. However, the effect is still not fully understood [2]. Figure 4 shows the effect of Na addition to an ADC12 (Al-Si-Cu) alloy.



**Figure 4.** Microstructures of an Al-Si-Cu alloy (ADC12) before and after the addition of 0.1% Na to modify the morphology of eutectic Si, reproduced from [42], with permission from Elsevier, 2022.

Sodium is one of the most potent modifiers but has conflicting effects. The addition of metallic Na to melted aluminum generates turbulence, which may lead to hydrogen absorption and oxidation [2,3]. It also suffers evaporation losses [2]. The excess of sodium, in addition to forming the AlNaSi phase, causes the increase of surface tension and reduction of melt fluidity. Strontium, although regarded as less effective, is less harmful in other senses [3]. Its addition changes the eutectic morphology from acicular to fibrous and accelerates Si spheroidization during solution treatment [16]. It also changes the previously described porosity distribution from macroscopic shrinkage voids to dispersed microporosity. Additionally, it has been shown that Sr can alter the morphology of the Mg<sub>2</sub>Si phase, converting it from fragmented to skeletal. In the presence of higher amounts of Mg, its modifying action can be limited by the formation of intermetallics containing Mg and Sr [7]. It might also increase porosity due to hydrogen uptake and surface tension effects [3]. Strontium's recovery is more predictable than sodium's, but the element is still susceptible to evaporation losses, especially when the melt faces longer holding times at high temperatures, according to Zhang et al. [43]. Therefore, it is essential to maintain Sr content within specified limits considering such loss.

Like sodium, the reason for strontium's modifying action is still unclear. However, the two most likely theories to explain such an effect are the restricted growth theory and the restricted nucleation theory. Non-modified Si present little or no twinning evidence, whereas Sr addition increases twin density. According to the restricted growth theory, the element is adsorbed by the liquid front of the eutectic, hindering the adhesion of Si atoms to the growing crystal, promoting twinning, which results in a fibrous structure, as proposed to explain sodium's action. The restricted nucleation theory states that Sr addition retards the agglomeration of Si atoms at temperatures close to that of nucleation, causing the morphological change. In terms of mechanical properties, the presence of

Sr per se does not appear to exert significant effects; however, the neutralization of the plate-like morphology results in the reduction of stress concentration, contributing to the strength, ductility and toughness improvement [7]. The Al-Sr system has two eutectic points on which master alloys are based. The most commonly used are based on the leaner eutectic composition, with 4.1% Sr. They are formed by  $\text{Al}_4\text{Sr}$  particles dispersed in an Al- $\text{Al}_4\text{Sr}$  matrix and undergo conventional dissolution, whose rate increases with temperature increase. The other composition, with 88% Sr, yields special master alloys containing primary Sr and an Al-AlSr eutectic, which undergo exothermal dissolution, whose rate increases with temperature decrease [16]. The combination of Na and Sr can enhance the modifying effect [3].

The necessary amount of Sr typically varies from 150–200 ppm for eutectic alloys cast in a permanent mold to slightly higher values for sand casting, with lower cooling rates, or for alloys with higher Si contents [2]. In general, alterations observed upon Sr addition, such as reduction of eutectic particle size and aspect ratio, increase of primary Si fraction and reduction of eutectic temperature, are observed until additions as high as 200 ppm [44]. In Al-Si-Mg-Cu alloys, the modification effect showed itself independent from Sr concentration between 212 and 270 ppm [45]. For the A356 alloy, typical additions are in the order of 120 ppm. However, in high-purity alloys, with P contents lower than 10 ppm, the optimum effect can be obtained with additions as low as 60–70 ppm [46]. Zhang et al. concluded that, for permanent-mold-cast A356, this content is about 100 ppm, whereas the same alloy cast in sand mold requires amounts higher than 180 ppm [43]. Strontium in excess reduces the alloy's quality index [46]. The effects of Sr additions of 47, 156 and 720 ppm to the A356 alloy are shown in Figure 5, evidencing the precipitation of coarse particles and a reduction of the modification effectiveness with excessive additions.

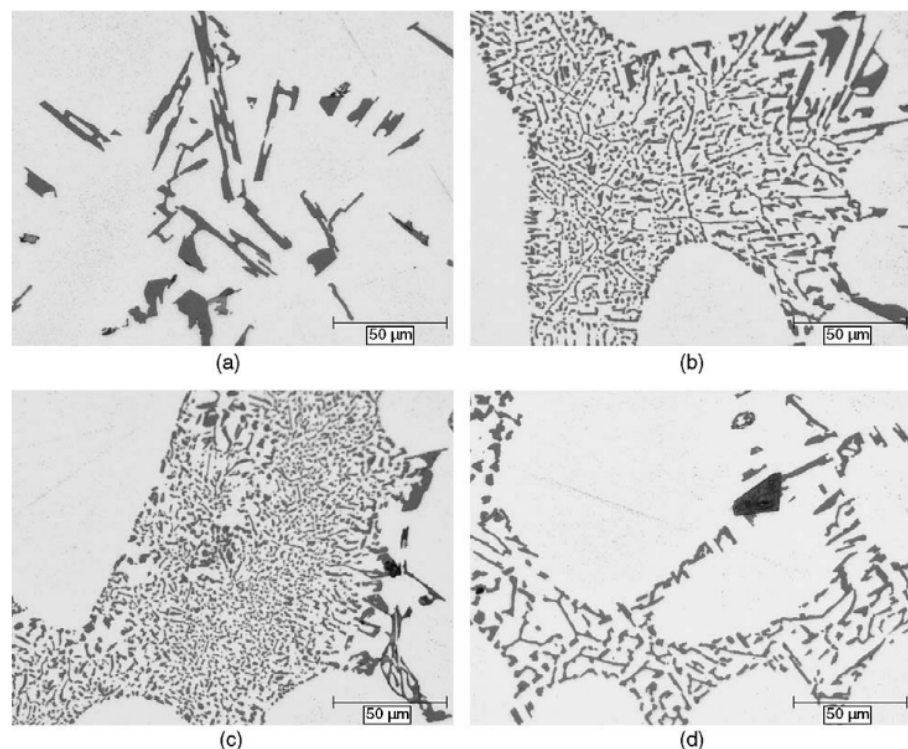


**Figure 5.** Morphologies of the eutectic phase in an A356 alloy: (a) without Sr addition; (b) with 47 ppm Sr; (c) with 156 ppm Sr; (d) with 720 ppm Sr, reproduced from [44], with permission from the Elsevier, 2016.

Fracchia, Gobber and Rosso observed, in Al-Si-Mg alloys with different Cu, Mn and Ni additions, that the interdendritic spacing is reduced with the addition of 250 ppm Sr, and the final values depend on the amount of silicon in the alloy. As for eutectic particle size,



before modification, there is considerable variation among all alloys, but upon Sr addition, value converges to an approximately linear relation with the amount of Si, with higher amounts resulting in larger particles. The eutectic phase fraction increased in all alloys after Sr addition. The higher concentration of alloying elements led to a reduction of impact energy absorption, while the addition of Sr caused an increase in the absorbed energy [47]. Regarding porosity, there are several hypotheses to explain the effect of Sr: reduction of eutectic temperature; alteration of the alloy's physical properties, specifically reduction of the gas/liquid interface energy and increase of volumetric shrinkage; an increase of hydrogen concentration in the melt due to an alteration of the absorption rate or solubility; influence in the formation of oxides, increasing their concentration in the oxide and/or the ability for pores to nucleate from oxides [7,48]. Studies indicate that Sr-rich particles nucleate on the wetted surface of the so-called bifilms, which consist of "folded" oxide layers formed during turbulent feeding with one internal, dry, oxide/oxide contact surface and one external, Al-wetted surface. This nucleation leads to the formation of SrO or  $\text{Al}_2\text{O}_3\text{-SrO}$ , meaning that a Sr oxide tends to be more porous than an Al one [49]. This strontium aluminate is regarded as less protective than aluminum oxide, which is supported by the respective Pilling–Bedworth ratios (PBR) of 0.65 and 1.29 for SrO and  $\text{Al}_2\text{O}_3$  [50] (one must remember that  $\text{PBR} > 1$  means that the oxide is prone to compressive residual stresses, whereas  $\text{PBR} < 1$  means a tensile stress state). For this reason, the compound is held responsible for an increase in hydrogen pick-up, although this effect is still a matter of dispute [7]. Wang, Hao and Yu observed an increase in the number of oxide inclusions in the A356 alloy with the increase of Sr amount [50], and Gyarmati et al. showed that Al-Si-Mg-Cu alloys with higher Sr content indeed present a higher amount of pores and higher bifilm content as well [51].

Antimony has a slightly different action, producing a lamellar morphology instead of fibrous [3,52]. Cai et al. attributed its modification effect to the precipitation AlSb compounds during solidification, which were absorbed in the growth front of the eutectic Si, inhibiting growth and thus refining Si particles [53]. It does not increase porosity like strontium. However, it has been verified that the impact toughness of A356 alloy is substantially enhanced by the addition of Sr, whereas the addition of Sb does not have significant effects on impact absorption properties [54]. On the other hand, an improvement of the corrosion resistance in saline solution has been attributed to Sb [55]. The beneficial effect of Sb is also reported in 319 alloys [52,56]. Its optimum amount might vary considerably depending on alloy composition and casting conditions, ranging from 0.009wt% [56] to 0.6wt% [53]. Likewise, bismuth (Bi) exerts the same effect on eutectic morphology and does not increase porosity. In an Al-15Si alloy, both Sb and Bi were effective as modifiers, but Bi caused superior improvement of mechanical properties [57]. However, the presence of Bi up to 200 ppm in a Na-modified A356 alloy caused coarsening of the eutectic Si phase due to an effect of increasing nucleation and growth temperatures of this phase, besides forming an Mg-Na-Bi intermetallic that reduces the efficiency of Na as modifier [58]. Scandium (Sc) addition also presents a certain modification effect [59], which is boosted in combination with zirconium (Zr) [19]. The addition of Sc, combined or not with Zr, is also effective in refining the primary Al phase, which makes it more advantageous when compared with Sr, as the latter does not have a proven microstructural refinement effect [19,59]. However, Ma et al. showed that, in terms of corrosion resistance, the combined addition of Sc and Zr is not beneficial: Sc alone did reduce corrosion rates in an Al-6.5Si-0.45Mg alloy, but the further introduction of Zr led to an increase in corrosion rates [19,60]. In the A356 alloy, Sc has also shown a modifying effect over Fe-rich phases  $\beta\text{-AlFeSi}$  and  $\pi\text{-AlFeMgSi}$ , in addition to preventing over-aging [61]. Finally, calcium (Ca) is considered a weak modifier, although its effects on eutectic modification, as well as refinement of Fe-rich phases and transformation of  $\beta\text{-AlFeSi}$  into  $\alpha\text{-AlFeSi}$ , have been recently reported in an A380 alloy [62].

As mentioned above, phosphorus is harmful to eutectic modification because it can form phosphides that compromise the effectiveness of modifiers. On the other hand,

in hypereutectic alloys, it constitutes the main addition to controlling the distribution and morphology of primary Si. Concentrations as low as 15 ppm are enough to achieve a sufficient modification effect [3]. Again, in the presence of Mg, the modifying effect of Sr can also be hindered by the reaction between said elements, which also results in a limitation of precipitation hardening during aging [63]. Antimony is also known for limiting the effectiveness of Sr, and boron (B) also poisons strontium's effect due to the formation of  $\text{SrB}_6$  [46]. The effects of Sb and P on the action of Sr are shown in Figure 6. Table 1 provides the results of works focused on the addition of eutectic modifiers to Al-Si alloys. Only the optimum compositions, i.e., compositions that resulted in the highest quality index (Q) are shown.

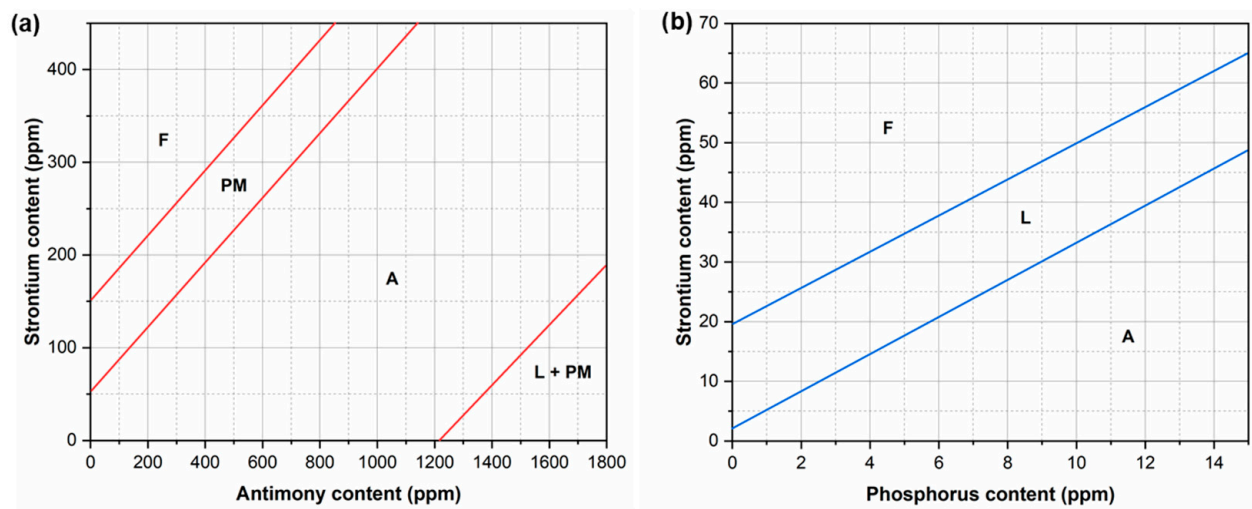


**Figure 6.** Effects of the interaction of elements with Sr on the eutectic morphology: (a) Antimony; (b) phosphorus. Diagrams provide domains of acicular (A), lamellar (L) and fibrous (F) morphologies, as well as of partial modification (PM) (data from [46]).

**Table 1.** Examples of results obtained by different authors whose works focused on the effects of the addition of eutectic modifiers to Al-Si-based alloys.

Optimized Alloy Composition (wt%)	Condition	UTS (MPa)	A (%)	Q (MPa)	Casting Technique	Ref.
Al-6.83Si-0.28Mg-0.10Fe-0.11Ti-0.003Cu-0.004Mn-0.023Sr-0.016B	T6	249.9	3.3	327.7	Permanent mold casting	[4]
Al-7.01Si-0.37Mg-0.08Fe-0.13Ti-0.01Sr	As cast	276.0	6.9	401.6	Permanent mold casting	[64]
Al-(9.0–11.0)Si-(0.20–0.45)Mg-0.55Fe-0.15Ti-0.45Mn-0.25AlSr10	As cast	320.0	8.0	455.5	Permanent mold casting	[65]
Al-15Si-1Bi	As cast	192.0	14.0	363.9	Permanent mold casting	[57]
Al-15Si-1Sb	As cast	203.0	9.2	347.6	Permanent mold casting	[57]

### 2.3. Grain Refiners

Apart from solidification conditions, grains' morphology also depends on alloy composition and the density of effective nucleation sites. The most common grain refiners are Al-Ti- or Al-Ti-B-based master alloys. Al-Ti alloys usually contain between 3% and 10% Ti, and the same concentration range is seen in Al-Ti-B alloys, with boron amounts of 0.2–1.0%. To be effective, grain refiners must form aluminides ( $\text{TiAl}_3$ ) or borides ( $\text{TiB}_2$ ) in controlled quantities, with size, morphology and distribution favorable to grain nucle-

ation [3]. Several theories were developed in an attempt to explain the action mechanism of the Al-Ti-B system. It is believed that  $TiB_2$  particles act as heterogeneous nucleation sites, and Ti atoms in solid solution, coming from the decomposition of  $TiAl_3$ , act as grain growth inhibitors [66]. On the other hand, the refinement effect is also attributed to  $TiB_2$  covered by a  $TiAl_3$  layer, onto which the matrix nucleates [67]. This  $TiAl_3$  layer reduces crystallographic misfit between Al's and  $TiB_2$ 's lattices from 4.22% to 0.09% [68]. The microstructure of the master alloy plays a key role in its performance, and the size of intermetallic particles varies considerably among different types of alloys. Overall, finer particles yield more efficient nucleating agents. However, alloy composition, especially regarding Ti content, also impacts its effectivity [66]. Figure 7 illustrates the refinement effect achieved after the addition of the master alloy.

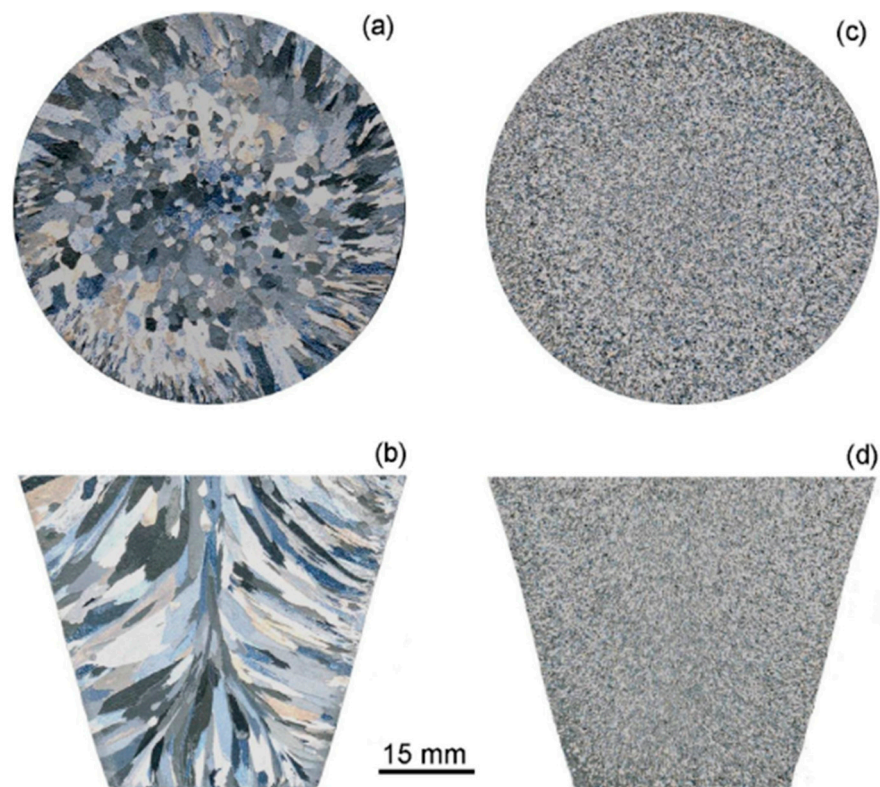


**Figure 7.** Grain structures of commercially pure Al: (a,b) before the addition of 0.2% Al-5Ti-1B refiner; (c,d) after the addition, reproduced from [67], with permission from the Elsevier, 2014.

The addition of Ti alone as a solute has little effect on grain size. Additionally, the addition of titanium can increase the cost of the alloy [16]. Furthermore, a work focused on the effect of the addition of Ti particles as reinforcement to an A356 alloy produced by compocasting has shown that excessive amounts of the element cause an expressive increase of porosity: in comparison with the Ti-free alloy (0.742% porosity), additions of 0.5%, 1.5% and 5% Ti resulted on porosity levels of 0.646%, 1.087% and 3.441%, respectively. Hardness increased continuously, but ductility and strength decreased with the excess of Ti. A maximum amount of 0.5% was considered ideal. The explanation provided was based on the formation of coarse agglomerates of particles and their action as pore nucleators due to the low wettability of liquid Al [69]. It has also been verified that the formation of  $TiAl_3$  particles by excess Ti hindered the wear resistance of eutectic Al-Si alloys, most likely due to the embrittlement effect and micro-cracking tendency resulting from the elevated hardness of particles [70]. In alloys with high Mg content (Al-6Mg-2Si), Ti addition has shown different effects, depending on the casting technique: in gravity casting, it slightly hindered mechanical properties, which was attributed to an alteration of the morphology of the  $Mg_2Si$  phase; in high-pressure die casting, however, properties were improved by

the addition of Ti, which was explained by an increase of the primary Al fraction and its consequent supersaturation [71]. Last but not least, the addition of Ti in excess can also be harmful to subsequent age hardening, forming Si-rich phases that limit its availability in solid solution to precipitate  $Mg_2Si$  during aging [16].

Despite that, the refinement effectiveness of  $TiB_2$  does depend on the presence of some Ti in excess. If excess boron is present in the alloy, it can react with other elements and form less effective compounds on the surface of  $TiB_2$  particles. Titanium excess, on the other hand, guarantees such effectiveness. As a rule of thumb, a minimum Ti:B ratio of 2 and a minimum Ti concentration of 0.1% are necessary for effective refinement [16], [66]. To avoid the need for Ti addition in solid solution, Al-Ti-B master alloys that comply with this limit should be preferred [16]. However, it has been shown that adding Al-B refiners to alloys with adequate prior Ti content also leads to effective refinement due to the reaction of boron with excess titanium to form  $TiB_2$  [72]. In an alloy A356 containing 0.06% Ti, the optimum amount of Ti added in the form of Al-Ti-B refiner ranged between 0.06% and 0.15%. Above this limit, deleterious effects on grain size and porosity were observed [73]. Apparently, grain refinement is intensified with additions up to 0.1% and, from this concentration on, grain size remains approximately constant. In Al-7Si alloys, higher amounts lead to a continuous increase in strength, but ductility is negatively affected [74].

Some elements, e.g., Si, Sc and Zr, can negatively affect (poison) the refinement effect of Al-Ti-B systems [16,75]. It is believed that the presence of Sc or Zr, for instance, leads to the formation of Ti-rich intermetallics, meaning that the amount of titanium in a solid solution is reduced [76]. Huang et al. also verified that Sc diffuses into  $TiB_2$  particles, hindering their effectiveness as nucleation sites [77]. When Si is present in concentrations higher than 3%, the effectiveness of the Al-5Ti-1B alloy is significantly reduced, but its poisoning mechanism is still not clear. One hypothesis states that, in the presence of high Si amounts, the element segregates to the  $TiB_2$ /Al interface, penetrating the  $TiAl_3$  layer and hindering the refinement effect [68]. Another theory involves the precipitation of silicides on the particles' surface, preventing Al nucleation due to the increase of crystallographic mismatch [68,75]. Samuel et al. recently suggested that  $TiAl_3$  loses its nucleation effectiveness in the presence of Si because they transform into silicides as well according to the following reaction:  $TiAl_3 \rightarrow Ti(Al,Si)_3 \rightarrow Ti(Al,Si)_2$  [72]. In a study about the poisoning effect of Si in an Al-13 Cu alloy, Jia et al. observed that the curvature radius of dendrites' tips in the Al-Cu-Si alloy was half the one observed in the Al-Cu alloy without Si. A sharper tip can disperse solute more effectively and grow faster [68].

The presence of  $TiB_2$  particles has also shown influence over the formation of porosity in Al-Si castings. An in situ observation of void formation in these alloys (Figure 8) demonstrated that the addition of Sr increases the amount of pre-existing bubbles in the semisolid region, while the addition of  $TiB_2$  without Sr makes pores more regular and apparently increases their formation temperature, but does not induce the formation of bubbles in the melt. The combined addition of Sr and  $TiB_2$ , in its turn, causes a significant increase in the size and quantity of bubbles and pores. The addition of Be, which can reduce the formation of oxides without significantly affecting the eutectic morphology modification, on the other hand, led to the formation of pores with regular morphology, smaller but in greater number, nucleating at temperatures lower to those observed after  $TiB_2$  addition, but higher than those experienced in the non-modified or Sr-modified alloy. Regarding strontium's effect on the eutectic temperature, its reduction provides more time for void growth. Despite that, the growth curve is dislocated to lower temperatures, resulting in no relevant alteration in pore size or fraction. Although no conclusion was drawn by authors about the effect of Sr on hydrogen absorption and solubility, the fact that its addition raises the temperature of the void formation above the *liquidus* temperature suggests that it might intensify pore nucleation due to oxide formation. The effect of grain refiner on the increase of pore density and nucleation temperature and decrease of pore size, with more homogeneous nucleation, can be explained by the fact that, as grain nucleant,  $TiB_2$  increases the fraction of equiaxed dendrites, among which pores can grow. This results

in a limitation of pore growth. The increase in nucleation rate and temperature can be attributed to the supersaturation of hydrogen in the liquid or to the possibility of  $\text{TiB}_2$  acting as a pore nucleation agent as well. When it comes to its combined action with Sr, the fact that together they increase the stability of pre-existing bubbles, while Be cancels this effect, suggests that both act in the formation of oxides, which constitute the main enablers for porosity formation. The higher pore density after Be addition might result from a lower nucleation temperature, leading to less time for hydrogen diffusion and pore coalescence, favoring a more homogeneous dispersion [48].

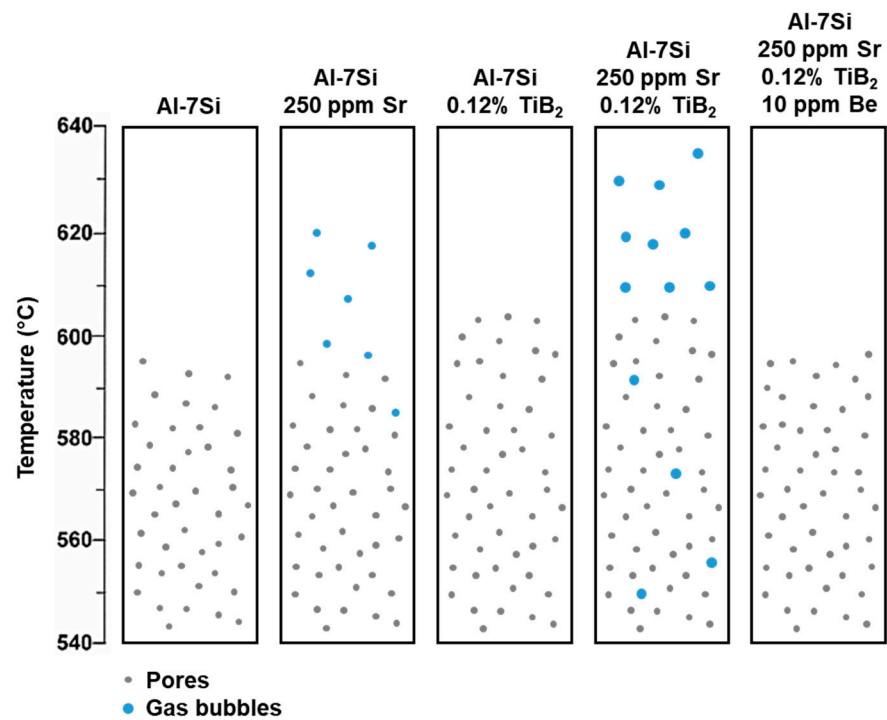


**Figure 8.** Void formation (pores and gas bubbles) in an Al-7Si alloy with different additions of Sr,  $\text{TiB}_2$  and/or Be (data from [48]).

With respect to oxide bifilms, the addition of Al-5Ti-1B refiner to the A356 alloy showed itself effective in reducing their amount.  $(\text{Al,Si})_3\text{Ti}$  particles nucleate on the wetted surfaces of bifilms and tend to decant towards the bottom of the crucible due to their higher density; in this process, oxide films tend to follow [78,79]. On one hand, such attachment is obviously advantageous to reduce bifilm content and porosity; on the other hand, Gyarmati demonstrated that these intermetallic particles could also bind to oxide layers on the surface of the melt, leading to a possible Ti segregation in the top region [79]. It is also advised that feeding of the melt takes place as rapidly as possible to avoid excessive decantation of the refiner, limiting its primary action. Therefore, there is an optimum holding time between addition and feeding to balance bifilm elimination and grain refinement effects. In the work of Gurtaran and Uludağ [80], the optimum holding time was 40 min.

The Al-Ti-B combination is the most common method for grain refinement in cast Al alloys. Nonetheless, other master alloys, such as Al-Ti-C and Al-Ti-C-B, have been suggested as alternatives to overcome the poisoning effect of certain elements on the refinement effect of the Al-Ti-B system. The C-containing alloy is also acknowledged for improving aluminum's castability. Although it is suggested that increasing holding time degrades refining action due to the decomposition of  $\text{TiC}$  particles into  $\text{Al}_4\text{C}_3$ , with subsequent growth [66], no negative effect was observed due to holding after the addition of an Al-3Ti-1B-0.2C refiner [81]. The use of an Al-2Ti-0.3C-0.2B master alloy containing C-doped  $\text{TiB}_2$  and B-doped  $\text{TiC}$  has shown itself effective against Si and Zr poisoning, even after long holding times, by B-TiC-assisted nucleation of Al grains on C- $\text{TiB}_2$  particles [82]. Another example of a master alloy is Al-10Sr-

2B (StroBor<sup>®</sup>), which may act both as a eutectic modifier and grain refiner. It does not contain titanium, relying on the fact that it is already present in many commercial alloys as a solute. Thus, boron present in the SrB<sub>6</sub> phase is dissolved after addition to form TiB<sub>2</sub>. In addition to SrB<sub>6</sub>, the alloy contains SrAl<sub>4</sub>, which acts on the modification of the eutectic morphology [66]. Scandium has also shown a certain refinement effect in Al-Si-Mg alloys, though not as effective as that of Ti. Its main mechanism consists of heterogeneous nucleation by the formation of the Al<sub>3</sub>Sc phase [83–85]. In an Al-7Si-0.25Mg alloy with 0.05% Sr and 0.36% Al-5Ti-1B, the addition of Sc in concentrations of 200–800 ppm resulted in a continuous increase of hardness and strength due to microstructural refinement [86]. Its addition to an A356 alloy also resulted in a fluidity increase and hot tearing reduction [87]. Nonetheless, Sc can form other intermetallic phases that do not act effectively as refiners, meaning that its use is not advised in highly alloyed systems [88]. Ding et al. developed a master alloy with the composition Al-9Zr-0.9Sr containing Al<sub>3</sub>Zr and Al<sub>4</sub>Sr. Its addition amounting to 3% to an Al-7Si-0.5Mg resulted in significant grain size reduction and eutectic morphology modification. Al<sub>3</sub>Zr reacts with Si, forming an AlSiZr-based phase that is much more stable and crystallographically similar to TiAl<sub>3</sub>, acting as a heterogeneous nucleation site. Meanwhile, Al<sub>4</sub>Sr dissolves, releasing Sr in a solid solution for the eutectic modification [89]. Cui et al. produced an Al-3B-5Sr master alloy, which acted very effectively as a grain refiner and eutectic modifier in the A356 alloy, most likely due to the precipitation of SrB<sub>6</sub>, as a result of the reaction between AlB<sub>2</sub> and dissolved Sr [90]. Recently, a new refiner, Al-3.5-FeNb-1.5C, has been tested in HPDC Al-Si-Cu alloys and showed significant refining effects when added at a concentration of 0.1%. Excessive additions, in the order of 1.0%, led to poor refining efficacy [91]. Latest developments include the fabrication and application of medium entropy metal diborides, (Ti<sub>1/3</sub>Cr<sub>1/3</sub>V<sub>1/3</sub>)B<sub>2</sub>, based on the tailoring of minimized lattice mismatch [92], and composite NaCl/KCl/K<sub>2</sub>TiF<sub>6</sub>/KBF<sub>4</sub> for simultaneous grain refinement (Ti-B) and eutectic modification (Na, K) [93], and as effective refiners for aluminum alloys.

Grain refiners based on niobium (Nb) have also been developed in the Al-Nb-B form, with analogous action to that of Al-Ti-B [94]. When added as a solute, Nb is not as effective for grain refinement either. However, when combined with boron, it forms the NbB<sub>2</sub> phase, which is more stable than its Ti-based counterpart, with the additional advantage of refining the eutectic phase as well. It becomes more effective for Si contents above 6% [95]. It was verified that the Nb-based refiner reduces undercooling levels, meaning that heterogeneous nucleation is the dominant mechanism [96]. The absence of interaction between Nb-B refiners and elements present in commercial alloys, such as A356, proves the chemical stability of Al<sub>3</sub>Nb and NbB<sub>2</sub> compounds, reducing poisoning effects [97]. The development of Al-Ti-Nb-B refiners confirmed that NbB<sub>2</sub> is very stable when facing higher Si amounts in an Al-10Si by the formation of NbB<sub>2</sub>-coated TiB<sub>2</sub> particles, that extinguishes Si poisoning due to a decrease of crystallographic mismatch and Si adsorption rate on the surface, and increase of chemical affinity with Al, as shown in Figure 9 [75]. The addition of Nb-B also apparently reduces the dependence of grain size on the cooling rate, making it more effective for different casting techniques [97]. It also prevents the formation of columnar grains upon slow cooling [96]. Another apparent benefit is the length reduction of the β-AlFeSi phase in Al-Si alloys with high Fe content [98]. However, the main refinement effect is observed in the primary dendrites of the matrix [97]. One disadvantage is the high density of Nb that results in a higher decantation tendency, reducing effectiveness with holding time. While the Al-Ti-B refiner is used with excess Ti to avoid the presence of free B, Wu et al. [75] produced an Al-3.5Nb-1Ti-1B refiner with an Nb:B ratio inferior to the stoichiometric one of 4.1:1 to avoid the presence of free Nb. Figure 10 shows the grain structure of Al-10Si alloy under the effect of different master alloys. Anyhow, Al-Ti-B remains the most widely used refiner for commercial applications [66]. Table 2 summarizes results of grain sizes obtained in different published works.

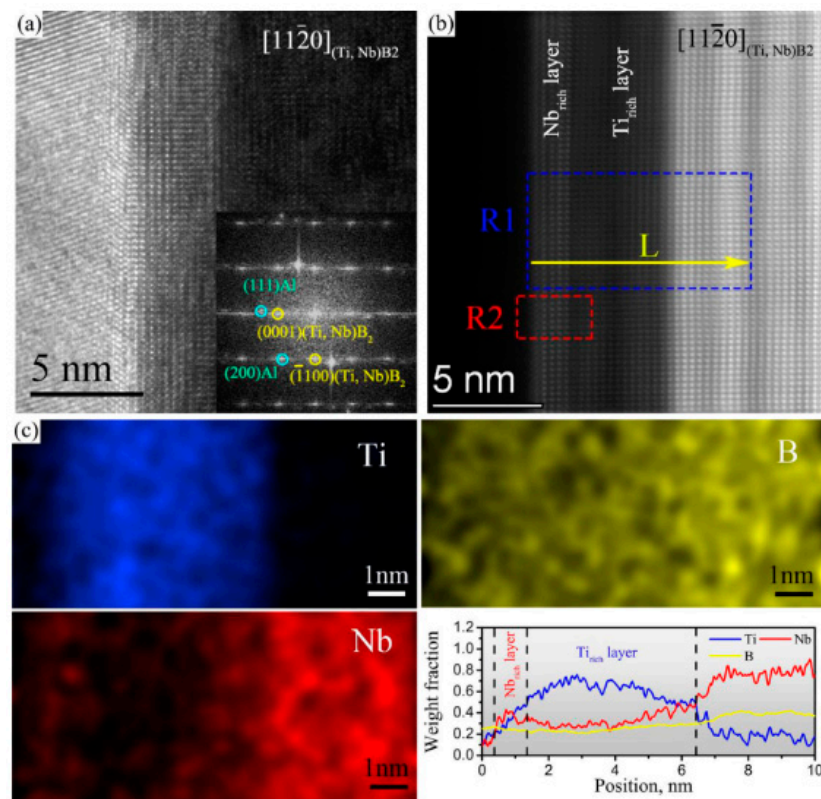


**Figure 9.** High-resolution transmission electron microscopy images showing the presence of an Nb-rich layer on the surface of  $\text{TiB}_2$  in an Al-3.5Nb-1Ti-1B alloy: (a) (0001)  $(\text{Ti, Nb})\text{B}_2$ /Al interface structure and corresponding fast Fourier transform (FFT) pattern; (b) high-angle annular dark-field (HAADF) image of the (0001)  $(\text{Ti, Nb})\text{B}_2$ /Al interface structure; (c) elemental maps of R1 region and line scan across L line, both shown in (b), reproduced from [75], with permission from the Elsevier, 2021.

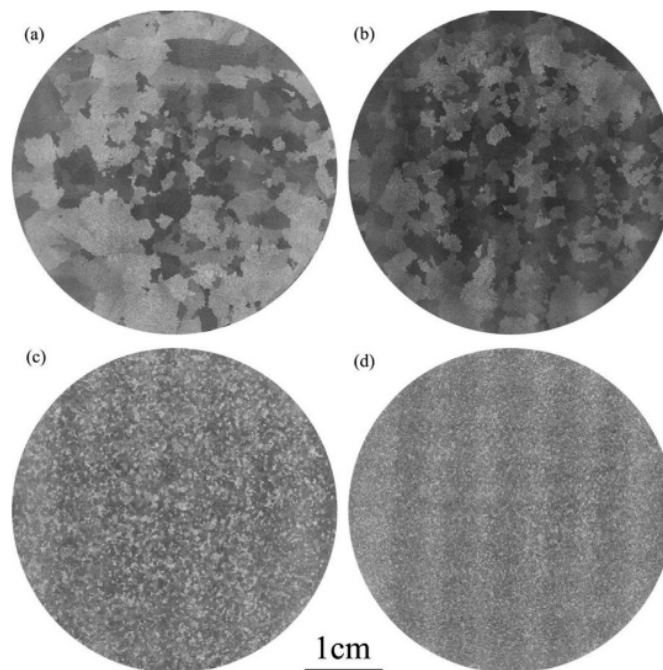


**Figure 10.** Grain structures of an Al-10Si alloy: (a) without refinement; (b) with Al-5Ti-1B addition; (c) with Al-4Nb-0.5B addition; (d) with Al-3.5Nb-1Ti-1B addition, reproduced from [75], with permission from the Elsevier, 2021.

**Table 2.** Examples of results obtained by different authors whose works focused on the effects of the addition of grain refiners to Al alloys.

Base Alloy Composition (wt%)	Optimum Grain Refiner Amount and Composition (wt%)	Average Grain Size ( $\mu\text{m}$ )	Casting Technique	Ref.
Commercially pure Al	2.7% ( $\text{Ti}_{1/3}\text{Cr}_{1/3}\text{V}_{1/3}$ ) $\text{B}_2$	35.0	N.A.	[92]
A356	0.5% Al-3B-5Sr	300.0	Permanent mold casting	[90]
A356	0.10% Nb as 96Al-2Nb-2B	150.0	Permanent mold casting	[96]
Al-1.0Si-0.3Mg	0.15Zr-0.30Sc	140.0	Permanent mold casting	[83]
Al-1.3Si-0.5Mg	0.15Zr-0.30Sc	219.0	Permanent mold casting	[83]
Al-4.02Si-0.02Fe	1.03Sc	31.7	Permanent mold casting	[85]
Al-6.0Si	0.10% Nb-KBF <sub>4</sub>	500.0	Solidification in glass wool-insulated graphite crucible	[95]
Al-(6–8)Si-0.3Mg-0.5Fe-0.11Ti-0.003Cu-0.005Mn-0.003Zn	0.10% Nb-KBF <sub>4</sub>	100.0	Solidification in glass wool-insulated graphite crucible	[97]
Al-6.83Si-0.34Mg-0.07Fe-0.11Ti-0.24Sr	0.20% Al-3Ti-1B-0.2C	167.0	Permanent mold casting	[81]
Al-6.96Si-0.13Fe-0.005Cu	0.10% Al-5Ti-1B	118.0	Permanent mold casting	[74]
Al-7.40Si-0.35Mg-0.34Fe-0.06Ti-0.08Cu-0.06Mn	0.15% Al-5Ti-1B	270.2	Permanent mold casting	[73]
Al-7.0Si-0.4Mg	0.10% Al-2Ti-0.2B-0.3C	85.0	Permanent mold casting	[82]
Al-7.0Si-0.5Mg	3% Al-9Zr-0.9Sr	122.0	Permanent mold casting	[89]
Al-7.0Si-1.0Fe	0.05% Al-4Nb-0.5B	104.0	Permanent mold casting	[94]
Al-9.0Si-1.0Fe	0.05% Al-4Nb-0.5B	120.0	Permanent mold casting	[94]
Al-12.0Si-1.0Fe	0.05% Al-4Nb-0.5B	222.0	Permanent mold casting	[94]
Al-5.0Cu-0.15Zr	0.50% Al-2Ti-0.2B-0.3C	63.0	Permanent mold casting	[82]

#### 2.4. Iron and Modifiers of the $\beta$ -AlFeSi Phase

The main disadvantage of Fe presence is the formation of intermetallic phases that can negatively affect the mechanical properties and castability of Al-Si alloys. Table 3 provides a summary of the several Fe-rich intermetallics that can be observed in these alloys, originally compiled in the work of Mbuya et al. [6], and Figure 11 presents some typical morphologies. The main ones are  $\beta$ -AlFeSi, with acicular or plate morphology;  $\alpha$ -AlFeSi (M)Si, with polyhedral or Chinese script morphology; and  $\pi$ -AlMgFeSi, with Chinese script morphology. The two priors will be discussed ahead, while the latter, already mentioned, forms in the presence of higher Mg contents. Iron does impart a few positive effects, such as high-temperature strength and hot tearing resistance, in addition to enhancing the refinement effect of Al-5Ti-1B, neutralizing the poisoning effect of elements such as zirconium (Zr), for instance. In lower concentrations, Fe itself might act as a refining agent. Nevertheless, its negative effects are much more prominent and critical [6].

**Table 3.** Fe-rich phases that can be present in cast Al-Si alloys, depending on the composition (data from [6]).

Morphology	Phase	Typical Conditions
$\beta$ —acicular	Al <sub>5</sub> FeSi (eutectic)	0.05% < Fe < 0.7%
	Al <sub>5</sub> FeSi (primary)	Fe > 0.7%
$\alpha$ —Chinese script	Al <sub>15</sub> Fe <sub>3</sub> Si <sub>2</sub>	Presence of Fe
	Al <sub>15</sub> (Fe,Mn) <sub>3</sub> Si <sub>2</sub>	Mn > 0.2% in the presence of Fe
$\pi$ —Chinese script	Al <sub>9</sub> FeMg <sub>3</sub> Si <sub>5</sub>	Presence of Mg and Sr
	Al <sub>8</sub> FeMg <sub>3</sub> Si <sub>6</sub>	Fe > Mg
	Al <sub>10</sub> FeMg <sub>4</sub> Si <sub>4</sub> / Al <sub>5</sub> FeMg <sub>8</sub> Si <sub>6</sub>	Presence of Mg



Table 3. Cont.

Morphology	Phase	Typical Conditions
Acicular	$\text{Al}_7\text{FeCu}_2$	Presence of Cu
	$\text{Al}_8\text{CuMg}_8\text{Si}_6$	$\text{Cu} > 1\%$ , $\text{Mg} > 2\text{xCu}$
Agglomerate	$\text{Al}_9\text{FeNi}$	$\text{Ni} > 0.1\%$ in the presence of Fe
	$\text{Al}_5\text{Cu}_2\text{Mg}_8\text{Si}_6$	Presence of Mg, Cu and Si
Chinese script	$\text{Al}_9(\text{Fe},\text{Co})_2$	$\text{Co} > 0.1\%$ in the presence of Fe
	$\text{Al}_8\text{Fe}_2\text{SiBe} / \text{Al}_4\text{Fe}_2\text{Be}_5$	Presence of Be
	$\text{Al}_5\text{Fe}_2\text{Si} / \text{Al}_8\text{Fe}_2\text{Si}$	Presence of Mg, Cu or Zn
Polyhedral	$\text{Al}_2(\text{Fe},\text{Cr})_5\text{Si}_8$	$\text{Cr} > 0.1\%$ in the presence of Fe
	$\text{Al}_{13}(\text{Fe},\text{Cr})_4\text{Si}_4$	$\text{Cr} > 0.1\%$ in the presence of Fe

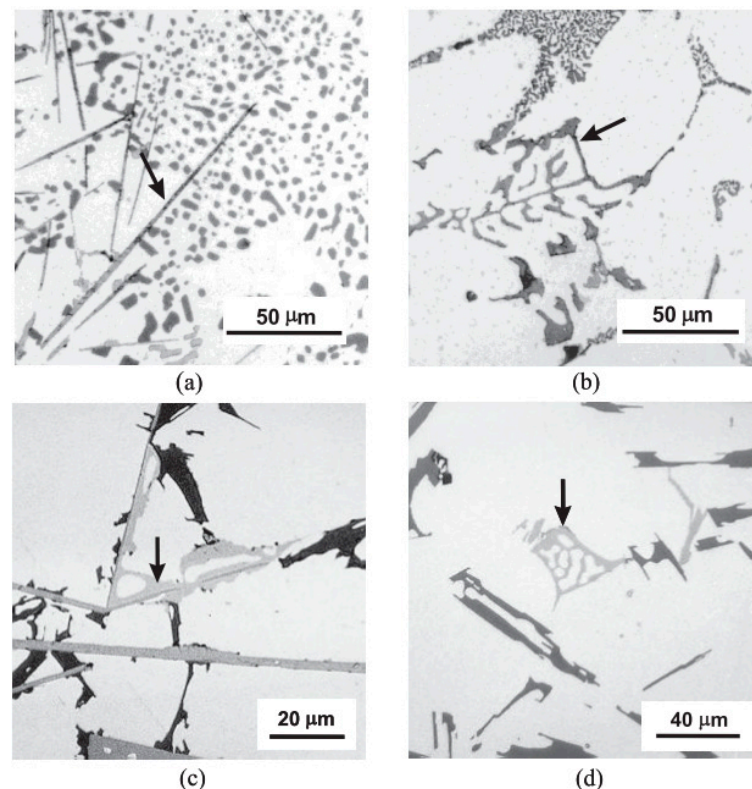


**Figure 11.** Morphologies of some Fe-rich phases observed in an Al-5Si-1Cu-0.5Mg alloy, indicated by arrows: (a) platelets of  $\beta\text{-AlFeSi}$ ; (b) Chinese script  $\alpha\text{-Al(Fe,M)Si}$ ; (c)  $\pi\text{-AlFeMgSi}$  growing from  $\beta\text{-AlFeSi}$ ; (d) Chinese script  $\pi\text{-AlFeMgSi}$ , reproduced from [99], with permission from Elsevier, 2012.

The  $\alpha\text{-AlFeSi}$  phase is identified as  $\text{Al}_8\text{Fe}_2\text{Si}$ ,  $\text{Al}_{12}\text{Fe}_3\text{Si}_2$  or  $\text{Al}_{15}\text{Fe}_3\text{Si}_2$ . There is no agreement about its crystal structure, which has already been described as body-centered cubic or hexagonal. It has a compact Chinese script or polygonal morphology and can precipitate either as a eutectic with the Al matrix or as a primary phase; the precipitation mechanism, as well as alloy composition, dictate its morphology. The  $\beta\text{-AlFeSi}$  phase is usually defined as  $\text{Al}_5\text{FeSi}$  or  $\text{Al}_9\text{Fe}_2\text{Si}_2$ . It does not have a well-defined crystal structure either, but a monoclinic structure is generally accepted, although orthorhombic and tetragonal structures have already been reported too. It is regarded as the most harmful Fe-bearing phase because of its needle- or plate-like morphology, which leads to stress concentration and brittleness [66]. It causes ductility, toughness and fatigue resistance reduction, and even strength reduction at times, in addition to affecting fluidity and feeding characteristics, by blocking interdendritic channels that allow the liquid to flow to empty regions. Its

particles also facilitate porosity formation [6]. They are known to nucleate on the wetted surface of bifilms, and upon their linear growth, the oxide films are also elongated, which helps to explain the negative effects of this phase on mechanical properties [66,100]. Due to its morphology,  $\alpha$ -AlFeSi is considered less harmful [66].

Considering the virtually inevitable presence of iron as an impurity, especially in recycled alloys, the most common strategy involves the addition of elements that can convert the critical  $\beta$ -AlFeSi into  $\alpha$ -AlFeSi, such as manganese (Mn), chromium (Cr) and cobalt (Co). However, one must bear in mind that these elements contribute to increasing the total amount of Fe-rich phases, which is, either way, undesirable [66]. Another disadvantage is that modified intermetallics tend to segregate and form coarse agglomerates [66]. In addition to these elements, several others, such as beryllium (Be), molybdenum (Mo), nickel (Ni), vanadium (V), tungsten (W) and the classical eutectic modifier, strontium, as well as rare earth (RE) elements, e.g., cerium (Ce), lanthanum (La), neodymium (Nd) and yttrium (Y), can be used to neutralize the deleterious effects of Fe-rich phases [6,66]. High melting point elements, such as Cr, Mo, V and W, are seldom used in Al-Si alloys due to their limited solubility in aluminum. On the other hand, they can also be useful for enhancing precipitation-hardening effects. These elements can form intermetallic phases that embrittle the alloy, especially under lower cooling rates during casting. Therefore, their addition is not recommended in alloys to be cast in sand or ceramic molds. In hypoeutectic alloys, the formation of precipitates with melting points higher than the crystallization temperature of Al changes the concentration profile in the solidification front. Under higher cooling rates, such as those experienced during HPDC, the solid solution can become supersaturated with these elements, contributing to the improvement of mechanical properties [101].

Manganese is widely used to minimize iron's effects due to its availability and low cost. Also, it has an atomic radius and crystal structure similar to those of Fe, making it possible for it to act as a substitutional element. In sufficient amounts, it favors the  $\alpha$ -Al(Fe,Mn)Si phase, with a typical composition of  $\text{Al}_{15}(\text{Fe,Mn})_3\text{Si}_2$ . However, compositions  $\text{Al}_{19}\text{Fe}_4\text{MnSi}_2$  or  $\text{Al}_{19}(\text{Fe,Mn})_3\text{Si}_2$  have also been observed. In Figure 12, the *liquidus* projections of ternary Al-Fe-Si and quaternary Al-Fe-Mn-Si (0.3 wt% Mn) are shown, where it is possible to observe the appearance of the  $\alpha$ -AlMnSi phase field in the presence of Mn. Polygonal, coarse dendritic or Chinese script morphologies can be attained, depending on the cooling rate and Mn:Fe ratio [66,102,103], as shown in Figure 13. The amount of Mn necessary to neutralize Fe is still not well established because such an effect also depends on other factors, such as the cooling rate, thermal history, heat treatment, initial amounts of Fe and Si and the presence of other elements [66,104]. As a general rule, a minimum Mn:Fe ratio of 0.5 is recommended, especially for iron contents above 0.45% [104]. In an Al-Si-Cu alloy containing 0.5% Fe, Mn additions up to 0.3% Mn were not enough to promote complete conversion. Upon addition of 0.65% Mn, conversion was complete, and mechanical properties were improved. For higher Mn contents, deterioration of mechanical properties took place due to the excess of intermetallic phases [105]. In an A356 alloy, microstructural refinement with a reduction of interdendritic spacing was observed after the addition of 0.5% Mn and Si content increase from 7% to 10%, leading to ductility and fatigue resistance improvement [106]. On the other hand, in the same alloy, Fortini et al. verified that Mn addition with Mn:Fe ratios varying between 0.37 and 1.11 did not exert any significant modification effect. Authors attributed this behavior to the low amount of Fe in the alloy, of about 0.1%, while the modifying effect should be intensified for higher Fe contents, especially above 0.2%. The addition of Mn resulted in the reduction of  $\beta$ -AlFeSi particles' density but not in their length reduction. The fact that this effect did not impact mechanical properties suggests they are sensitive to particle length and insensitive to number density [30]. In an A356 alloy with iron contents of 0.123, 0.454 and 0.655% and Mn addition, Kuchariková et al. observed that increasing Fe content does not necessarily result in the continuous lengthening of  $\beta$ -AlFeSi particles, but rather in their thickening, and such thickening leads to increased porosity. However, there is a tendency for length increase in comparison with lower Fe contents. The authors did not observe a concrete negative

effect on mechanical properties arising from increased Fe content due to dispersion of results, i.e., the variation among the alloys lies within the error intervals. Nevertheless, in general terms, the best values for strength, elongation, hardness and fatigue properties were verified in the alloy with the highest critical Fe concentration ( $Fe_{crit} = 0.075 \times Si - 0.05$  [99]), and the highest yield strength was observed in the alloy with the highest Mn:Fe ratio. For  $\beta$ -AlFeSi particles shorter than 50  $\mu\text{m}$ , fatigue properties depended strongly on the porosity size, but for longer particles, properties began to depend on their length [107]. In eutectic Al-Si alloys, it is suggested that Mn addition leads to the fragmentation of  $\beta$ -AlFeSi platelets in concentrations up to 0.9% and, above that, converts the morphology into a dendritic one [100]. The addition of manganese to modify  $\beta$ -AlFeSi also contributes to the reduction of porosity in the presence of high Fe contents [108].

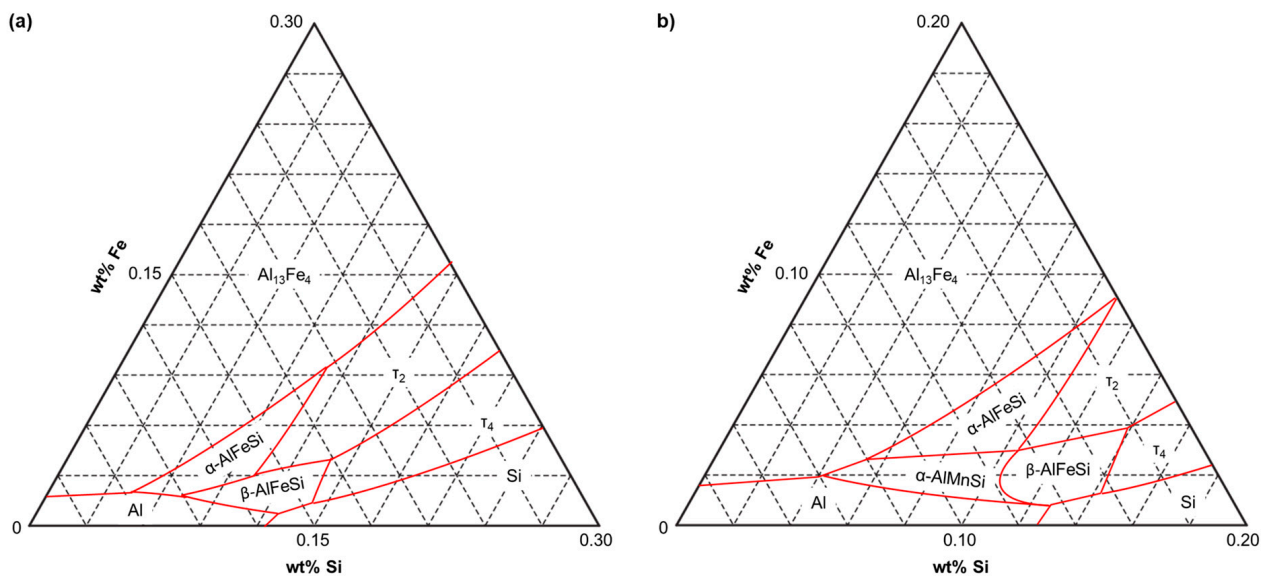


**Figure 12.** Liquidus projections of the Al-rich corners of (a) Al-Fe-Si system and (b) Al-Fe-Mn-Si system with 0.3% Mn (data from [109]).

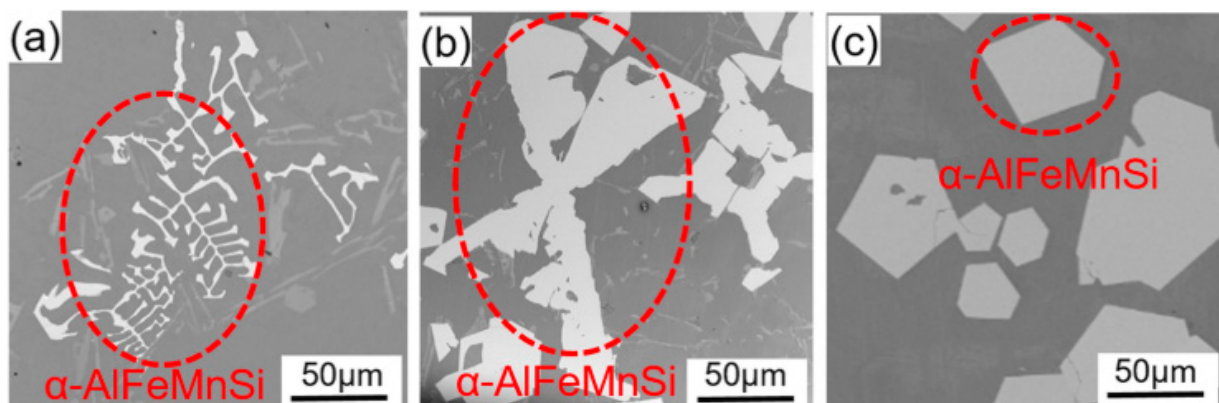


**Figure 13.** Morphologies of the  $\alpha$ -AlFeMnSi in an Al-7Si-0.3Mg-0.5Fe with different Mn contents: (a) 0.48%; (b) 0.77%; (c) 1.04%, reproduced from [102], with permission from Elsevier, 2022.

Alternatively, Cr and Co can also be employed for this purpose. Like Mn, both possess atomic radii close to iron's radius, and Cr also has the same crystal structure as Fe. However, there are fewer reports about the effects of these elements. Especially with respect to chromium, its amount is usually limited by the sludge factor ( $SF = 1 \times Fe + 2 \times Mn + 3 \times Cr < 1.7$  [99,110,111]) due to its and manganese's tendency to form coarse sludge particles together with Fe. Cobalt is considered less effective than

Mn but, on the other hand, less harmful. Chromium is considered more effective, being used with Cr:Fe ratios above 0.33 [66]. The element can also increase precipitation hardening [55]. One supposed advantage of Co is favoring the precipitation of  $\alpha$ -Al(Fe,M)Si phase within Al dendrites, reducing segregation tendency. As for Cr, the phase can precipitate both inside dendrites and on their boundaries [104]. Wang et al., nonetheless, compared the effects of Mn, Cr and Co as neutralizers in an Al-Si-Cu alloy and observed that cobalt forms a high melting point intermetallic,  $\text{Al}_7(\text{Fe},\text{Co})\text{Cu}_2$ , which also presents a plate-like morphology and has a negative effect on mechanical properties [112]. In A356 alloy, the combined addition of 0.13% Mn and 0.13% Cr showed itself more effective than the single addition of 0.2% Mn because, although strength levels were similar, ductility in the first case was much more improved [113]. In an Al-7Si-3Mg containing ~0.5% Fe, the addition of 0.45% Cr led to an improvement of strength, followed by a significant ductility reduction due to the precipitation of the  $\text{Al}_{13}\text{Cr}_4\text{Si}_4$  phase [114]. In the absence of Fe, the addition of 0.5% Cr to an A356 alloy reinforced with 5%  $\text{TiB}_2$  led to the precipitation of the  $\text{Al}_{13}\text{Cr}_4\text{Si}_4$  phase, whose particles acted as growth inhibitors for primary Al and the eutectic phase, contributing to microstructural refinement. In a corrosive environment, this phase can be dissolved to promote the formation of a passive film that significantly enhances corrosion resistance [115]. Ling et al. observed the formation of Chinese script  $\text{AlCrFeSi}$  phase upon the addition of 0.1–0.3% Cr to an Al-7Si-0.35Mg alloy, with further precipitation of  $\text{Al}_{13}\text{Cr}_4\text{Si}_4$  during aging as well [116]. The refining action of Cr in an A356 alloy has been further evidenced by Liang et al., according to whom such effect results from the high stability of the  $\text{Al}_{13}\text{Cr}_4\text{Si}_4$  / Al interface, owing to the low crystallographic mismatch and to the existence of certain orientation relationships between both phases [117]. In Al-Si-Cu-Mg-Ni alloys, the addition of 0.8% Fe and 0.5% Cr resulted in the precipitation of  $\alpha$ -Al(Fe,Cr)Si phase that induced the formation of a full or partially interconnected eutectic structure, as opposed to the dispersed distribution in the base alloy, due to the occurrence of secondary eutectic reactions. Such morphology alteration was essential to significantly improve the high-temperature properties of the alloy [118]. In a continuously cast AA6061 alloy, the addition of Cr in concentrations as low as 0.07% led to dendritic refinement, which was attributed to the precipitation of  $\text{Al}_{45}\text{Cr}_7$  phase, a potential heterogeneous nucleation site for primary Al grains. This led to a reduction of the flow tendency of primary liquid and of the semi-solid zone, decreasing the amount of residual liquid in central regions and thus the segregation level. After the T6 temper, both strength and ductility were increased, which was attributed to restricted segregation, grain refinement and precipitation of the  $\alpha$ -Al(Fe,Cr)Si phase [119]. In HPDC Al-Si-Cu alloys, it was verified that the presence of Mn, Cr and Fe did not have any significant impact on the heat-treatment response [39]. Table 4 summarizes optimized mechanical properties obtained by different authors upon optimized neutralization effects achieved by Mn and/or Cr.

**Table 4.** Examples of results obtained by different authors whose works focused on the effects of the addition of neutralizers of the  $\beta$ -AlFeSi phase to Al-Si-based alloys.

Optimized Alloy Composition (wt%)	Condition	UTS (MPa)	A (%)	Q (MPa)	Casting Technique	Ref.
A356-0.2Fe-0.13Mn-0.13Cr	T6	280.0	11.8	440.8	Permanent mold casting	[113]
Al-0.7Si-1.2Mg-0.1Fe-0.07Cr	T6	338.0	18.0	526.3	Twin-roll casting	[119]
Al-6.5Si-0.45Mg-0.5Fe-3.75Cu-0.65Mn	T6	460.0	0.5	408.0	Sand casting	[105]
Al-7.45Si-2.84Mg-0.50Fe-0.11Cu-0.13Ti-0.14Mn	As cast	350.0	3.1	423.7	Permanent mold casting	[114]
Al-9.5Si-0.35Mg-0.12Fe-0.13Ti-0.5Mn	T6	275.0	8.0	410.5	N.A.	[106]

Beryllium is considered more effective than the previous elements, being used in concentrations ranging between 0.06 and 0.27%, although the need for amounts higher than 0.4% has also been reported. Be-rich phases tend to precipitate inside dendrites, favoring toughness. The addition of Be modifies the ternary eutectic reaction that originates  $\beta$ -AlFeSi, giving place to a peritectic reaction [66]. It has also been observed that the presence of Be appears to induce the precipitation of  $\beta'$  (Mg-Si) particles with fine globular or acicular morphologies during aging, which is also beneficial for mechanical properties [25]. The major disadvantage of Be is its toxicity [6].

The addition of elements such as Cr, Mo and W to an Al-9Si-3Cu-1Fe in controlled amounts (0.2% Cr or 0.5% Mo/W) resulted in the primary crystallization of the  $\alpha$ -Al(Fe,M)Si phase, where M = Cr, Mo or W. The addition of vanadium (V), however, did not cause such an effect. Additionally, these elements promoted an increase in the *liquidus* temperature. Both the primary formation of the  $\alpha$  phase and the supersaturation of the Al matrix with them, enabled by a relatively high solidification rate, were held responsible for the enhanced mechanical properties of the produced alloys [101]. Although the effect of  $\alpha$ -AlFeSi formation was not observed upon vanadium addition in this work, other authors verified that the element does have a certain effect of modification of the  $\beta$ -AlFeSi phase in A356 alloy. Ludwig, Schaffer and Arnberg showed that the continuous addition of V up to 0.8% resulted in an enrichment of the phase with the element, and such enrichment was accompanied by a morphological alteration from acicular to polyhedral. However, in excess of 0.2%, the element also causes the precipitation of the Si<sub>2</sub>V phase with a polyhedral morphology. They highlight that vanadium is present in coke used as anode for the production of primary, being, therefore, likely present as an impurity in the alloy. This means that the comprehension of its effects on the metallurgy of Al alloys is important [120]. Lin et al. also noted benefits upon V additions up to 1% regarding the control of deleterious Fe-rich phases in the alloy, including reduction of the length of  $\beta$ -AlFeSi needles, increase in volume fraction of  $\alpha$ -AlFe(M)Si, porosity reduction and grain size reduction. Optimum effects were verified upon the addition of 0.8% V [121].

Although less used, molybdenum (Mo) can also act for the modification of the  $\beta$ -AlFeSi phase [66]. In an Al-10Si-0.65Mg-0.5Mn, the addition of 0.2% Mo increased *liquidus* temperature and solidification interval but resulted in the formation of the Chinese script  $\alpha$ -AlFe(Mn,Mo)Si phase, with partial substitution of Fe with Mo together with Mn [122]. Microstructural refinement is reported with concentrations up to 0.3% [55]. In Al-Si alloys, Mo in concentrations of 0.05–0.3% in combination with sulfur (S) in concentrations of 0.01–0.2% is acknowledged to improve mechanical properties [104]. A report also exists on the action of sulfur alone on the shape and distribution of the  $\alpha$ -Al(Fe,Mn)Si, promoting a dendritic script-like morphology [52]. On the other hand, the addition of Mo in an A354 alloy (Al-Si-Cu-Mg) caused a heterogeneous Sr distribution and increased porosity. The influence on Sr distribution, with consequent heterogeneity of eutectic morphology modification, was not elucidated, while porosity increase as attributed to a likely presence of oxides in the Al-Mo master alloy. Furthermore, the element led to the suppression of  $\beta$ -AlFeSi formation but, on the other hand, caused the precipitation of coarse intermetallic particles. After T6 heat treatment, precipitation of nano-sized Mo-bearing phases, but no significant improvement in mechanical properties was achieved due to the adverse effects previously described [123]. Strontium itself, in addition to modifying the eutectic morphology, can also promote suppression of the deleterious effects of the  $\beta$ -AlFeSi phase, either by favoring the precipitation of the Chinese script  $\alpha$ -AlFeSi phase or by refining the needle-like structure of the first. Suppression effects attained by the combination of Sr with P have also been reported [66]. In Al-Si-Mg alloys with Cu, Mn and Ni additions, the introduction of Sr led to a reduction of the area fraction of  $\beta$ -AlFeSi [47].

### 2.5. Rare Earth (RE) Elements

Master alloys containing RE elements have also been developed for application in Al alloys. Most compositions contain around 10% RE, close to the eutectic composition of the

majority of Al-RE binary systems [66]. The addition of rare earth promotes the formation of thermally stable intermetallics that, when dispersed in the matrix, contribute to microstructural refinement, with reduction of secondary dendritic arm spacing (SDAS), modification of eutectic morphology and grain boundary strengthening, leading to enhancement of high-temperature strength [124]. Eutectic modification by rare earth elements has been explained on the basis of the impurity-induced twinning (IIT) mechanism, which proposes that modifying atoms are absorbed on the {111} steps of the growing Si crystal, leading to the formation and growth of twins along {112} directions. This theory states that the ideal ratio between atomic radii of the element and of Si is close to 1.646, and this ratio varies between 1.5 and 1.7 for all REs. However, RE elements were also observed to increase the solidification interval in Al-Si alloys, in addition to reducing the nucleation temperature of the eutectic phase and increasing undercooling [125]. The use of RE can also reduce the tendency of hot tearing susceptibility during casting [126]. Adding rare earths can also bring positive effects to corrosion resistance because they form stable, protective oxides on the surface of the part [18,127].

In A356 alloy, the addition of 3.5% mischmetal (mixture of rare earth elements typically containing lanthanum, neodymium, praseodymium, cerium and iron impurities) led to expressive increases, higher than 100%, in the high-temperature strength. On the other hand, the ductility of the alloy underwent a significant decrease. These effects are attributed to the precipitation of thermally stable precipitates of  $\text{AlSiRE}$  and  $\text{Al}_{20}\text{Ti}_2\text{RE}$ , which are extremely hard and brittle, acting as stress concentration features, thus hindering elongation. The application of T6 temper did not have any relevant impact on the morphology of intermetallics, contributing only to the eutectic globularization. Upon the addition of rare earth, a higher amount of the  $\pi$  phase was also observed, which is more stable at higher temperatures than  $\text{Mg}_2\text{Si}$ , another characteristic that might have led to the high-temperature strengthening of the alloy [128]. Zhu et al. also studied the effects of mischmetal addition in an A356 alloy and observed that the optimum concentration of RE to maximize strength and elongation was 0.7% [129]. In an A356.2 alloy with 2, 4 and 6% mischmetal with and without Sr modification, it was verified that, in the non-modified alloy, the increase of RE content results in negligible hardness variation, whereas upon Sr modification, the hardness of the alloy decreases significantly with the addition of mischmetal. The peak hardness in all cases is achieved after aging at 180 °C; nonetheless, hardness levels are higher in the alloy without rare earth addition or Sr modification. The behavior of the alloy was explained on the basis that Sr is a more effective modifier than rare earth, and both cause a reduction of the eutectic temperature, increasing undercooling levels and shifting the eutectic point to higher Si concentrations, increasing the fraction of the ductile Al matrix. Behaviors during aging were attributed to a possible interaction of Mg with rare earth elements, meaning that less magnesium is available as solute to form the isothermal  $\text{Mg}_2\text{Si}$  phase [124]. The limited hardening of Cu-bearing alloys containing RE is also observed due to their interaction with the element [130]. It is also believed that rare earth reduces the diffusion rates of Cu and Mg, thus limiting the hardening effect of these elements during aging [131].

The addition of lanthanum ( $\text{AlLa}_{12}$ ) and scandium ( $\text{AlSc}_{2,2}$ ) in concentrations of 0.25% to an Al-(9.0–11.0)Si-(0.20–0.45)Mg alloy led to noticeable increases in hardness and ductility of the alloy, although strength increase was not as pronounced [65]. In an Al-10Si-2Cu alloy, the optimum concentration of La from the viewpoint of hardness and corrosion resistance was 0.6% [132]. A study on the addition of La and Sc to an Al-4.8Cu has shown that amounts of 0.4% of both elements exerted expressive effects on strength and ductility increase [133]. In a hypoeutectic Al-7Si alloy [134] and in an Al-5Mg-2Si-0.6Mn alloy [135], the optimum amount of La for property enhancement was 0.1%; higher additions led to the precipitation of coarse and embrittling intermetallics. In an A357 alloy, the optimum amount of cerium added was 0.16%. At this concentration, the element led to maximization of strength and ductility, owing to the formation of Ce-rich intermetallics that contributed to grain size and SDAS reduction, modification of eutectic morphology

and partial modification of the  $\beta$ -AlFeSi phase. In excess, however, the element contributes neither to microstructural refinement nor to the improvement of mechanical properties [136]. The optimum combined addition of Ce with ytterbium (Yb), known to promote eutectic modification, to an Al-6Si-0.6Mg-0.6Cu-0.2Cr alloy was 0.4% [137]. At concentrations up to 0.1%, the addition of europium (Eu) to an A356 alloy also led to microstructural refinement and considerable enhancement of mechanical properties. The element was acknowledged to increase undercooling for nucleation and growth during solidification. Its effect on Si morphology modification was attributed to the restricted growth theory due to the accumulation of Eu-rich clusters along the  $\langle 112 \rangle$  Si growth direction and at the intersection of  $\langle 111 \rangle$  Si twins [138]. In an Al-5Si-1.5Cu-0.4Mg alloy, the addition of 0.15% gadolinium (Gd) or ytterbium (Yb) combined with 0.15% Zr resulted in significant improvement of yield strength at room temperature and at 200 °C due to the formation of Al-Si-Yb and Al-Si-Cu-Gd phases and to the precipitation of  $(\text{Al,Si})_3\text{Zr}$  during homogenization (495 °C/3 h) [139]. Li et al. studied the effect of combined additions of 3.6% Mg and 0.5% La to a eutectic Al-Si alloy. The amount of Mg was calculated in order to fully convert the acicular  $\beta$  phase into the Chinese script  $\pi$  phase, whereas La was used for eutectic modification. Upon solution treatment at 560 °C/6 h,  $\pi$  phase underwent fragmentation and growth. The successful conversion of the  $\beta$  phase contributed significantly to improve mechanical properties and the resulting quality index [140].

Qiu et al. assessed the modification effect in an A356 alloy with the addition of a master alloy with the composition Al-6Sr-7La in an amount of 0.5%. As compared with the non-modified variation, the alloy conventionally modified with Al-5Ti-1B and Sr presented increases of 7.9% in strength and 114.2% in elongation. When the new master alloy was used, increases were 22.9% and 226.6%, respectively, leading to a significant elevation of the alloy's quality index. Beneficial effects were credited to a decrease in SDAS values combined with eutectic morphology modification. Additions higher than 0.5% of the master alloy, however, led to worsening of properties and reduction of quality index [141]. Likewise, Wu et al. produced an Al-5Sr-8Ce master alloy and verified that its addition to a level of 0.4% resulted in beneficial microstructural refinement and eutectic modification; in higher amounts, no positive effect was noted [142]. More recently, Ding et al. showed the benefits of adding 0.2% Al-3Ti-4.35La to an Al-7Si alloy due to eutectic modification, which was attributed to the impurity-induced twinning mechanism (IIT) [143]. Luo et al. demonstrated the beneficial effects of the addition of 500 ppm La + 200 ppm B + 150 ppm Sr to an Al-10Si alloy, with simultaneous grain refinement and eutectic modification, resulting in enhanced strength and ductility [144]. Nevertheless, comparing the isolated effects of Sr and La, minimum additions of 1% La are necessary to obtain modifying effects comparable to those achieved by the addition of 0.01% Sr in A356 alloy [64].

When Sr is present in solution in Al-Si alloys, the addition of La and Ce negatively affects the eutectic modification effect due to a possible reaction between Sr and these elements. This effect can be partially counteracted by higher La additions since it can also modify the eutectic phase, in addition to acting as grain refiner; as a downside, excessive lanthanum additions lead to the precipitation of coarse intermetallics harmful to the alloy's properties [130,145]. In the presence of Sr, the application of adequate solution treatments may cause fragmentation of these intermetallics [130,146]. Also, upon higher cooling rates, La and Ce, just like Mo and Zr, can form fine particles that contribute actively to the alloy's hardening. In work on the effect of the addition of these elements to an Al-Si-Mg-Zn alloy, the addition of Mo and Zr led to increased strength and hardness, and the later addition of La and Ce further improved these properties [147]. The addition of La and Ce to the A356 alloy was also acknowledged to increase the solidification interval, hindering the feeding of the melt [146]. Table 5 lists the optimum results of works by several authors whose focus was the addition of rare earth to Al alloys.

**Table 5.** Examples of results obtained by different authors whose works focused on the effects of the addition of rare earth to Al alloys.

Optimized Alloy Composition (wt%)	Condition	UTS (MPa)	A (%)	Q (MPa)	Casting Technique	Ref.
A356-0.5(Al-6Sr-7La)	As cast	230.0	12.0	391.9	Permanent mold casting	[141]
A356-0.4(Al-5Sr-8Ce)	T6	280.0	10.0	430.0	Permanent mold casting	[142]
Al-2.05Si-5.16Mg-0.62Mn-0.09La	As cast	275.0	5.5	386.1	Squeeze casting	[135]
Al-5.98Si-0.63Mg-0.13Fe-0.62Cu-0.19Cr-0.22Ce-0.17Yb	T6	336.8	7.5	468.1	Permanent mold casting	[137]
Al-6.9Si-0.29Mg-0.099Fe-0.18Ti-0.7MM <sup>1</sup>	T6	285.0	10.3	436.6	Permanent mold casting	[129]
Al-6.98Si-0.35Mg-0.08Fe-0.13Ti-0.99La	As cast	273.0	6.9	399.0	Permanent mold casting	[64]
Al-7.0Si-0.1La	T6	350.2	12.8	516.0	Permanent mold casting	[134]
Al-7.0Si-0.2(Al-3Ti-4.35La)	As cast	178.0	12.0	339.9	Permanent mold casting	[143]
Al-(9.0–11.0)Si-(0.20–0.45)Mg-0.55Fe-0.15Ti-0.45Mn-0.25AlLa12	As cast	230.0	8.2	367.1	Permanent mold casting	[65]
Al-9.65Si-0.61Mg-0.12Fe-0.31Mn-0.15Mo-1.04Zn-0.13Zr-0.06La-0.06Ce	Aged	362.0	3.8	449.0	High-pressure die casting	[147]
Al-10.0Si-0.015Sr-0.02B-0.05La	As cast	200.0	5.5	311.1	Permanent mold casting	[144]
Al-(12.54–12.68)Si-(3.52–3.63)Mg-(0.78–0.82)Fe-(0.47–0.54)La	T6	312.0	4.3	406.7	Permanent mold casting	[140]
Al-7.17Si-0.474Mg-0.135Fe-0.142Ti-0.023V-0.16Ce	T6	325.0	4.5	423.0	Permanent mold casting	[136]
Al-7.1Si-2.9Mg-0.16Fe-0.095Eu	T6	265.0	14.7	440.1	Permanent mold casting	[138]
Al-4.85Cu-0.38La	As cast	175.0	10.5	328.2	Permanent mold casting	[133]
Al-4.78Cu-0.37La-0.42Sc	As cast	225.0	9.0	368.1	Permanent mold casting	[133]

<sup>1</sup> MM: mischmetal.

## 2.6. Other Transition Elements

Transition elements, e.g., hafnium (Hf), scandium (Sc), titanium (Ti), vanadium (V) and zirconium (Zr), show potential for high-temperature strength improvement in cast Al alloys [148]. In a cast and hot-isostatically-pressed 356 alloys, the addition of 0.5% Cu + 0.15% Ti + 0.15% Zr + 0.25% V, together with eutectic modification by 150 ppm Sr, led to significant improvements in ultimate and yielded strengths of the alloy, both at room and high (237 °C) temperatures. At room temperature, yield strength increased from 210 MPa to 268 MPa, while ultimate strength was raised from 224 MPa to 279.3 MPa. At high temperatures, yield strength went from 122 MPa to 167 MPa and ultimate strength from 149 MPa to 186 MPa. In both cases, however, the strength increase was accompanied by a decrease in elongation, most likely due to the presence of hard, brittle phases that bring the benefit of being stable at higher temperatures [149]. Since all elements were added together, it is difficult to understand the contribution of each one separately. However, at least in an Al-Cu 224 alloy with individual and combined additions of Ti, Zr and V, Zr + V and Ti + Zr + V presented the best performance both at room and high (300 °C) temperatures, with the addition of Zr, in general, providing the best effect of  $\theta'$  stabilization at high temperatures [150].

Zirconium is usually added together with scandium to promote the formation of stable (Sc,Zr)Al<sub>3</sub> precipitates [151]. In an A356 alloy, the addition of the element in concentrations between 0.1 and 0.3% led to grain refinement due to the precipitation of ZrAl<sub>3</sub> particles prior to the solidification of the Al matrix, acting as heterogeneous nucleation sites for the matrix. Additionally, although not as effective as the  $\beta''$  phase for hardening purposes, ZrAl<sub>3</sub> particles do not grow as much as  $\beta''$  particles at temperatures around 150 °C, being useful, therefore, to maintain the hardness of the alloy constant at higher temperatures [152]. An addition of 0.1% Zr to an Al9SiMg alloy also resulted in a significant improvement in castability, although the effect on mechanical properties was not as significant [153]. Just as hafnium, Zr forms Si<sub>2</sub>X (X = Hf, Zr) dispersoids that are thermally stable, leading to the



enhancement of fatigue strength and creep behavior at high temperatures [148,154,155]. However, the addition of both elements combined to an Al-7Si-0.3Mg alloy resulted in a worsening of high-temperature strength [148]. In an Al-10Si-0.65Mg-0.5Mn, the addition of 0.2% Zr increased the liquid temperature and solidification interval and led to the precipitation of needle-like Zr-enriched phases. Alone, it exerted a negative impact on mechanical properties, especially ductility. However, when combined with 0.2% Mo, which acted to suppress the formation of  $\beta$ -AlFeSi and promote the formation of  $\alpha$ -Al(Fe,Mn,Mo)Si, it did not hinder the alloy's properties [122]. Moreover, in an Al-8Si-0.3Mg, it was observed that the combined additions of Zr, Mo and V (between 0.15 and 0.33%) led to increases as high as 27%, 32% and 61% in yield strength, ultimate strength and elongation, respectively [156].

In combination with erbium (Er), the addition of Zr to the A356 alloy brought improvement to high-temperature properties, specifically regarding creep, in addition to increasing the maximum hardness achieved by the alloy after aging [157,158]. Huang et al. observed both  $\text{Si}_2\text{Zr}$  and  $(\text{Al,Si})_3\text{Zr}$  dispersoids in an Al-7Si-0.3Mg alloy with 0.16% Zr, to whom an improved creep performance was attributed [159]. Isolated, it has been verified that the addition of 0.3% Er to an A356 alloy is also helpful in improving mechanical properties due to the precipitation of fine  $\text{ErAl}_3$  particles, the consequent microstructural refinement and an effect of suppression of the  $\beta$ -AlFeSi phase [160]. In an Al-11.5Si-4Cu alloy, it was verified that the addition of 0.2% Zr contributes more effectively to the improvement of strength at room temperature. Nonetheless, at high temperatures, Zr causes overaging, while Mn retards this effect, meaning that this element contributes more effectively to the thermal stability of the alloy, preventing strength reduction at higher temperatures [161]. In 224 (Al-Cu) alloys, the combined additions of V and Zr have shown themselves greatly beneficial to mechanical properties, both at room and high temperatures (300 °C) [151].

In Al-Cu alloys containing Mn, Mg and Ti, scandium and silver (Ag) additions led to an expressive microstructural refinement, with Sc acting more effectively than Ag on grain refinement. While the addition of silver caused higher strength and lower ductility levels due to the stronger contribution of the  $\Omega$  phase precipitation to hardening, the addition of Sc resulted in a significant ductility increase combined with lower strength levels [162]. In an A357 alloy cast in sand and metal molds, the addition of 0.5% Sc led to a more significant reduction of grain size after sand casting, while the effect on SDAS was more notable in the metal-cast condition. Regarding mechanical properties, the element induced the increase of ultimate strength and yield strength after T6 treatment, the latter particularly expressive in the sand-cast condition, meaning that Sc reduces the sensitivity of these properties to the cooling rate. Ductility, on the other hand, was significantly improved in the alloy cast in metal mold due to SDAS reduction [163]. The addition of 0.2% Sc to an Al-11.5Si-4Cu also showed itself effective in improving high-temperature strength, mainly due to the promotion of  $\theta'$  and  $\theta''$  precipitation during aging, as well as improvement of thermal stability of these phases, preventing their transformation into  $\theta$ . Furthermore, the element provided a refinement effect and the suppression of  $\beta$ -AlFeSi, which was replaced by (Fe,Sc)-rich phases [164].

The adequate addition of nickel (Ni), as well as Mg and Cu, and the application of heat treatments, can increase mechanical strength, wear resistance and even ductility of Al-Si alloys due to solid solution hardening [165]. Also, the addition of Ni is believed to improve corrosion resistance [55]. In an HPDC A384 alloy, the addition of 0.2% Ni led to the best strength-ductility combination, while an amount of 0.5% Ni caused the maximization of age hardening [166]. In Al-Si-Mg-Cu alloys containing Zr, additions of Ni and Mn resulted in strength improvement, but ductility's behavior did not present any clear trend. Higher Ni additions (4%) and the combination of Mn and Ni (0.75% + 2%) led to ductility losses. After T6 treatment, the combined addition did not result in a strength gain as high as those achieved upon the isolated addition of these elements. In these conditions, improvements can be attributed to the presence of phases such as  $\text{Al}_3\text{Ni}$ ,  $\text{Al}_9\text{FeNi}$ ,  $\text{Al}_3\text{CuNi}$  and  $\text{Al}_{15}(\text{Fe,Mn})_3\text{Si}_2$  and to the formation of fine precipitates after heat treatment. In excess, nonetheless, these phases become harmful to mechanical properties. Also, the presence of

excessive Ni consumes all Cu available to form  $\text{Al}_3\text{CuNi}$ , thus limiting the precipitation of  $\theta'$  during aging [167].

In A356 alloy, nickel's effect appears to depend on the composition of the alloy and on solidification conditions. Lattanzi et al. observed that the addition of Ni in amounts between 0.5% and 2% continuously decreases strength, both in as-cast and T6 conditions. Authors attributed strength reduction to the inability of the network formed by eutectic Si and Ni-rich intermetallics to act as effective obstacles to crack propagation. The fragile behavior of the alloy increased with the increase in Ni concentration [168]. On the other hand, upon Sr modification of a Ti-bearing A356 alloy, Ozyurek et al. observed that Ni addition in amounts up to 1% led to strength improvement with a slight reduction of ductility in the T6 condition. This concentration of the element promoted a homogeneous morphology distribution of eutectic Si, while higher additions caused the phase to agglomerate. The fracture was caused mainly by Ni-rich intermetallics [169]. Strength evolution as a function of Ni amount in both studies is shown in Figure 14. As compared with Cu at the same concentration levels in Al-7Si alloys, both non-modified and modified with 200 ppm Sr, Ni does not appear to increase ultimate strength as effectively but does increase yield strength. The impact of Ni on ductility is stronger than that of Cu [170].

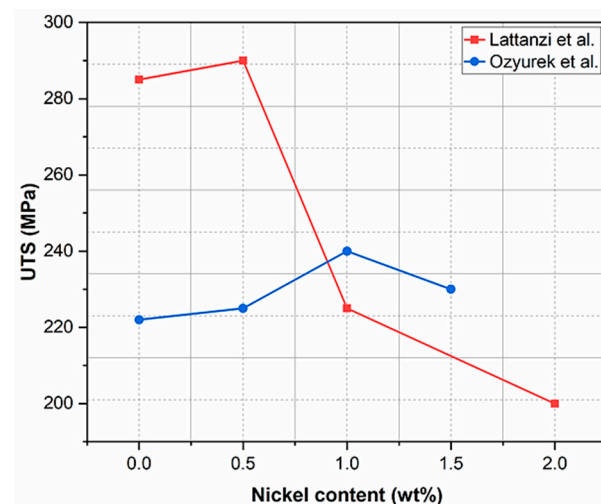


**Figure 14.** Results of ultimate tensile strength (UTS) obtained of A356 alloy as function of Ni content obtained by different authors (data from [168,169]).

Casari et al. evaluated the influence of Ni (600 ppm) or V (1000 ppm) addition on tensile and impact properties of the A356 alloy without grain refinement or eutectic modification. In sand-mold-cast conditions, both elements led to increased strength after the T6 temper treatment, whereas the addition of Ni led to a strength decrease and the addition of V led to a strength increase in the as-cast condition. After casting in a permanent mold, no significant influence was detected [171]. Regarding impact toughness, both Ni and V additions led to enhanced energy absorption after sand casting in as-cast and T6 conditions. When cast in a permanent mold, the as-cast alloy presented lower toughness after the addition of both elements but higher toughness after the T6 temper [172]. In an HPDC A360 alloy, the addition of V in amounts between 0.1 and 0.7% resulted in dendritic refinement but led to higher levels of microstructural heterogeneity. The higher the microstructural refinement effect, the worse the tensile and impact properties of the alloy, meaning that V addition also possesses an embrittling effect. The addition of 200 ppm Sr managed to counteract these effects, promoting slight increases in strength, ductility and toughness, while additions of 0.02–0.2% B resulted in a strength decrease, but ductility and toughness were considerably enhanced [173]. In a 6101 alloy, the addition of Ni as an alternative to Mn and Cr led to the transformation of the  $\beta$ -AlFeSi phase into an Al-Fe-Si-Ni intermetallic with rod-like morphology, and the optimum amount of Ni added

to the alloy was 0.2%, while higher additions resulted in limited ductility [174]. From the viewpoint of corrosion, the effect of 0.5% Ni addition to an Al-7Si-0.35Cu-0.25Zn-0.6Fe was time-dependent: for short measurements, the Ni-bearing alloy showed lower corrosion resistance; however, after long exposure (30 days), the formation of an alumina layer enriched with Ni on the surface led to a significant improvement [175].

Elements such as tin (Sn) and zinc (Zn) do not appear to perform any beneficial effect on the properties of HPDC Al-Si-Cu alloys. Zn promotes negligible solid solution strengthening when Mg content is lower, but it also accelerates softening due to over-aging at high temperatures, and Sn also hinders castability. Therefore, their concentrations in the alloy should be minimized [39]. With respect to corrosion resistance, Zn addition to Al-Si-Cu has shown to firstly reduce corrosion rates due to the formation of a protective oxide layer over Al<sub>2</sub>Cu particles and then exert the opposite effect in amounts above ca. 1% due to the alteration of the morphology of these particles [176]. In 7xxx series' alloys, increasing Zn concentration between 5 and 11% resulted in higher hot tearing susceptibility and melt viscosity, besides increasing strength at the expense of a ductility reduction [177].

The addition of indium (In) to an Al-Si-Cu alloy resulted in a maximum hardness increase after aging, with a reduction of the time needed to achieve such hardness. Indium nanoparticles were present in an amount more than twice that of Al<sub>2</sub>Cu precipitates, with sizes significantly smaller as compared with those observed in the alloy without the element, meaning that In nanoparticles can act as heterogeneous nucleation sites [178]. In HPDC alloys, the combined additions of Mg and germanium (Ge) accelerated the aging response due to the formation of intermetallic phases [179]. In Al-Si-Cu-Mn-Ni alloys, the addition of 200 ppm B altered the morphology and refined the primary Al<sub>3</sub>MnSi<sub>2</sub> phase, being the effect attributed to the formation of borides that also acted as nucleation sites [180]. Adding proper amounts of yttrium (Y), as well as Ni, Ti and Cu, can improve hot tearing susceptibility due to the precipitation of Y-rich phases that lead to the reduction of the solidification interval. However, results have shown that hot tearing susceptibility firstly decreases but then increases as Y concentration is continuously increased in an Al-4.4Cu-1.5-Mg-0.15-Zr. The optimum amount of yttrium regarding hot tearing in the alloy was of 0.15%. Above that, in addition to increasing hot tearing susceptibility, the element also promotes microstructural coarsening, and the effect of reduction of the solidification interval is damped. The deleterious role of excessive Y can be explained by the precipitation of coarse (Al,Y)-rich particles that tend to agglomerate, hindering feeding of liquid metal [126]. Table 6 summarizes optimized compositions obtained by the addition of transition elements and their respective properties.

**Table 6.** Examples of results obtained by different authors whose works focused on the effects of the addition of various elements to Al alloys.

Optimized Alloy Composition (wt%)	Condition	UTS (MPa)	A (%)	Q (MPa)	Casting Technique	Ref.
Al-0.42Si-0.58Mg-0.19Fe-0.097Cu-0.20Ni	HO <sup>1</sup> + CR <sup>2</sup> + T6	240.0	14.8	415.5	Permanent mold casting	[174]
Al-6.67Si-0.53Mg-0.19Fe-0.16Ti-0.56Cu-0.12Mn-0.07Cr-0.22V-0.10Zr-0.0156Sr	As cast	145.0	7.8	278.8	Permanent mold casting	[122]
Al-7.01Si-0.62Mg-0.04Fe-0.08Ti-0.53Sc	T6	384.0	11.3	542.0	Permanent mold casting	[163]
Al-7.68Si-0.30Mg-0.14Fe-0.05Ti-0.51Mn-0.15Mo-0.25V-0.19Zr-0.012Sr	T6	214.4	5.0	319.2	Permanent mold casting	[156]
Al-8.33Si-0.36Mg-0.25Fe-0.096Ti-0.134Cu-0.27Mn-0.014Cr-0.12Zn-0.30Zr	As cast	164.2	1.6	194.8	Sand casting	[153]

Table 6. Cont.

Optimized Alloy Composition (wt%)	Condition	UTS (MPa)	A (%)	Q (MPa)	Casting Technique	Ref.
Al-9.77Si-0.63Mg-0.13Fe-0.059Ti-0.46Mn-0.20Cr-0.19Mo-0.22Zr	As cast	142.0	7.9	276.6	Permanent mold casting	[122]
Al-10.1Si-0.65Mg-0.13Fe-0.066Ti-0.52Mn-0.19Cr-0.20Mo-0.003Zr	HIP <sup>3</sup> + T6	279.3	4.4	375.8	Permanent mold casting	[149]
Al-(9.0–11.0)Si-(0.20–0.45)Mg-0.55Fe-0.15Ti-0.45Mn-0.25AlSc2.2	As cast	235.0	8.6	375.2	Permanent mold casting	[65]
Al-11.5Si-0.30Mg-0.74Fe-3.82Cu-0.21Mn-0.28Ni-0.02Sr	T6	429.9	3.6	513.9	High-pressure die casting	[166]
Al-6.64Si-0.24Mg-0.08Fe-0.44Ni	T6	287.0	N.A.	N.A.	Permanent mold casting	[168]
Al-7.18Si-0.33Mg-0.59Fe-0.11Ti-1.05Ni-0.020Sr	T6	240.0	6.0	356.7	Sand casting	[169]
Al-6.9Si-0.34Mg-0.087Fe-0.061Ni-0.007V	T6	284.8	3.3	361.6	Permanent mold casting	[171]
Al-6.99Si-0.35Mg-0.094Fe-0.003Ni-0.108V	T6	289.5	3.6	372.9	Permanent mold casting	[171]
Al-4.78Cu-0.37La-0.42Sc	As cast	225.0	9.0	368.1	Permanent mold casting	[133]

<sup>1</sup> Homogenized; <sup>2</sup> Cold rolled; <sup>3</sup> Hot-isostatically pressed.

### 3. Concluding Remarks

An overview of the studies focused on the microstructural modification of hypoeutectic casting Al alloys, mainly Al-Si-based, by the addition of various alloying elements, has been provided. The primary conclusion to be drawn is that a given element hardly ever presents an invariable effect on the microstructure and properties of these alloys. Firstly, because other elements can be present in the alloy, each with their own characteristics, and with whom these intended additions, at times, will inevitably interact. These interactions can be either beneficial or harmful. Furthermore, casting conditions, e.g., pouring temperature, holding time, solidification rate, casting practices (filtering, cleanliness, turbulence), as well as heat treatment conditions, can directly impact the quality of the final component and also play key roles in the consolidation of the microstructure.

Nevertheless, some specific trends can be observed:

- With respect to optimization of the morphology of eutectic Si, strontium addition remains the main route for achievement, usually at amounts no higher than 200 ppm to avoid issues related to porosity and coarse precipitate formation, although the use of antimony has also been a matter of interest, although an excessively wide range of Sb concentration in Al alloys has already been assessed and, in general, these are higher than the ones necessary for Sr. The use of alkaline metals, such as sodium and calcium, does not appear to be advantageous.
- Regarding grain refinement, Al-5Ti-1B master alloy remains the material of choice to achieve this goal, usually added in amounts up to 0.15wt%. However, the interest in the development of other refiners that can overcome the poisoning effect to which the Ti-B-based ones are susceptible in certain compositions, as well as the idealization of master alloys with multiple actions, e.g., grain refinement + eutectic modification at one, is pointed out. In this sense, the development of Al-Ti-C-B-based, Nb-based and RE-based systems is noteworthy, as well as all of them being added in similar

concentrations as those used for the Al-Ti-B-based ones. Rare earth elements still bring the additional advantage of improving the corrosive properties of Al alloys.

- To overcome the deleterious effect of the needle-shaped  $\beta$ -AlFeSi phase, the addition of manganese appears to be the most straightforward solution, especially considering the low cost and availability of the element. Despite the existence of the Fe:Mn = 2:1 rule of thumb, relatively high Mn concentrations, around 0.1–0.2%, have been successfully used. Other elements—Cr, Mo, V, W, Ni—can also perform this neutralizing action. The challenge remains to define optimum amounts to be added to the alloy to ensure that the deleterious phase is completely neutralized without the formation of intermetallic phases in excess and too coarse, which can be equally harmful to the alloy's performance. This is a matter of vital importance, especially considering the increasing recycling trend since recycled Al alloys usually present even higher Fe amounts.
- Several elements, especially transition elements and rare earth, can be used for the purpose of improving strength and thermal stability. Again, careful design of these additions is necessary to avoid the formation of coarse precipitates and aggregates that provide no tangible benefit to the final material. Promising transition elements include nickel, vanadium, scandium and zirconium, whose optimum amounts will rely on base alloy composition and desired properties. Their effects on corrosion are disputed and appear to depend on exposure conditions in addition to element concentration. The relevance of studies focused on thermal stability justifies itself by the increasing interest in critical applications of Al alloys in the automotive and aerospace sectors to maximize weight reduction.
- Studies focused on the careful design of alloying elements' amounts are necessary to help overcome cost-related issues, provided that several of the promising elements, such as niobium, rare earth and transition elements, are relatively expensive. In this sense, property optimization can counteract economic issues by allowing the use of less material and reduced sections in components to achieve similar strength levels.

**Author Contributions:** Conceptualization, B.C., T.N.L. and R.S.C.; methodology, B.C. and T.N.L.; formal analysis, B.C.; investigation, B.C.; resources, R.S.C.; data curation, B.C.; writing—original draft preparation, B.C.; writing—review and editing, B.C., T.N.L. and R.S.C.; visualization, B.C.; supervision, R.S.C.; project administration, T.N.L.; funding acquisition, R.S.C. All authors have read and agreed to the published version of the manuscript.

**Funding:** This research received no external funding.

**Data Availability Statement:** Not applicable.

**Conflicts of Interest:** The authors declare no conflict of interest.

## References

1. Rams, J.; Whittaker, M. (Eds.) Light Alloys and Composites—High Temperature Extreme Alloys and Composites. In *Encyclopedia of Materials: Metals and Alloys*; Elsevier: Amsterdam, The Netherlands, 2022; Volume 1.
2. Polmear, I.; StJohn, D.; Nie, J.-F.; Qian, M. *Light Alloys: Metallurgy of the Light Metals*, 5th ed.; Elsevier: Amsterdam, The Netherlands, 2017.
3. Kaufman, J.G.; Rooy, E.L. *Aluminum Alloy Castings: Properties, Processes, and Applications*, 1st ed.; ASM International: Amiel, The Netherlands, 2004.
4. Kaba, M.; Donmez, A.; Cukur, A.; Kurban, A.F.; Cubuklusu, H.E.; Birol, Y. AlSi<sub>5</sub>Mg<sub>0.3</sub> Alloy for the Manufacture of Automotive Wheels. *Int. J. Met.* **2018**, *12*, 614–624. [[CrossRef](#)]
5. Glazoff, M.V.; Khvan, A.V.; Zolotarevsky, V.S.; Belov, N.A.; Dinsdale, A.T. *Casting Aluminum Alloys: Their Physical and Mechanical Metallurgy*, 2nd ed.; Butterworth-Heinemann: Oxford, UK, 2018; ISBN 9780128121146.
6. Mbuya, T.O.; Odera, B.O.; Ng'ang'a, S.P. Influence of Iron on Castability and Properties of Aluminium Silicon Alloys: Literature Review. *Int. J. Cast Met. Res.* **2003**, *16*, 451–465. [[CrossRef](#)]
7. Ganesh, M.R.S.; Reghunath, N.; J. Levin, M.; Prasad, A.; Doondi, S.; Shankar, K.V. Strontium in Al–Si–Mg Alloy: A Review. *Met. Mater. Int.* **2022**, *28*, 1–40. [[CrossRef](#)]
8. Hiremath, P.; Sharma, S.; Shettar, M. Influence of Various Trace Metallic Additions and Reinforcements on A319 and A356 Alloys—A Review. *Cogent Eng.* **2022**, *9*, 2007746. [[CrossRef](#)]

9. Dash, S.S.; Chen, D. A Review on Processing-Microstructure-Property Relationships of Al-Si Alloys: Recent Advances in Deformation Behavior. *Metals* **2023**, *13*, 609. [[CrossRef](#)]
10. Campbell, J. A Personal View of Microstructure and Properties of Al Alloys. *Materials* **2021**, *14*, 1297. [[CrossRef](#)] [[PubMed](#)]
11. Abdel-Jaber, G.T.; Omran, A.M.; Khalil, K.A.; Fujii, M.; Seki, M.; Yoshida, A. An Investigation into Solidification and Mechanical Properties Behavior of Al-Si Casting Alloys. *Int. J. Mech. Mechatron. Eng.* **2010**, *10*, 30–35.
12. Bogdanoff, T.; Seifeddine, S.; Dahle, A.K. The Effect of Si Content on Microstructure and Mechanical Properties of Al-Si Alloy. *Metall. Ital.* **2016**, *108*, 65–68.
13. Wang, Y.; Liao, H.; Wu, Y.; Yang, J. Effect of Si Content on Microstructure and Mechanical Properties of Al-Si-Mg Alloys. *Mater. Des.* **2014**, *53*, 634–638. [[CrossRef](#)]
14. Cáceres, C.H.; Taylor, J.A. Enhanced Ductility in Al-Si-Cu-Mg Foundry Alloys with High Si Content. *Metall. Mater. Trans. B* **2006**, *37*, 897–903. [[CrossRef](#)]
15. Kumar, V.; Mehdi, H.; Kumar, A. Effect of Silicon Content on the Mechanical Properties of Aluminum Alloy. *Int. Res. J. Eng. Technol.* **2015**, *2*, 1326–1330.
16. Lumley, R.N. (Ed.) *Fundamentals of Aluminium Metallurgy: Production, Processing and Applications*; Woodhead Publishing: Siston, UK, 2011.
17. Garc, C.; Isabel, A.; Mart, F. Comparative Study on Microstructure and Corrosion Resistance of Al-Si Alloy Cast from Sand Mold and Binder Jetting Mold. *Metals* **2021**, *11*, 1421. [[CrossRef](#)]
18. Gomes, L.F.; Kugelmeier, C.L.; Garcia, A.; Della Rovere, C.A.; Spinelli, J.E. Influences of Alloying Elements and Dendritic Spacing on the Corrosion Behavior of Al-Si-Ag Alloys. *J. Mater. Res. Technol.* **2021**, *15*, 5880–5893. [[CrossRef](#)]
19. Ma, Y.; Liu, Y.; Wang, M. Microstructures and Corrosion Resistances of Hypoeutectic Al-6.5Si-0.45 Mg Casting Alloy with Addition of Sc and Zr. *Mater. Chem. Phys.* **2021**, *276*, 125321. [[CrossRef](#)]
20. Osório, W.R.; Goulart, P.R.; Garcia, A. Effect of Silicon Content on Microstructure and Electrochemical Behavior of Hypoeutectic Al-Si Alloys. *Mater. Lett.* **2008**, *62*, 365–369. [[CrossRef](#)]
21. Öztürk, İ.; Ağaoglu, G.H.; Erzi, E.; Dispinar, D.; Orhan, G. Effects of Strontium Addition on the Microstructure and Corrosion Behavior of A356 Aluminum Alloy. *J. Alloys Compd.* **2018**, *763*, 384–391. [[CrossRef](#)]
22. Abalymov, V.R.; Zhereb, V.P.; Kleimenov, Y.A.; Antonov, M.M. Effect of Heat Treatment on the Structure and Mechanical Properties of Eutectic Silumin Alloyed with Magnesium. *Met. Sci. Heat Treat.* **2021**, *63*, 291–296. [[CrossRef](#)]
23. Wang, B.; Zhang, M.; Wang, J. Quantifying the Effects of Cooling Rates and Alloying Additions on the Microporosity Formation in Al Alloys. *Mater. Today Commun.* **2021**, *28*, 102524. [[CrossRef](#)]
24. Dinnis, C.M.; Otte, M.O.; Dahle, A.K.; Taylor, J.A. The Influence of Strontium on Porosity Formation in Al-Si Alloys. *Metall. Mater. Trans. A* **2004**, *35*, 3531–3541. [[CrossRef](#)]
25. Elsharkawi, E.A.; Ibrahim, M.F.; Samuel, A.M.; Doty, H.W.; Samuel, F.H. Understanding the Effect of Be Addition on the Microstructure and Tensile Properties of Al-Si-Mg Cast Alloys. *Int. J. Met.* **2022**, *16*, 1777–1795. [[CrossRef](#)]
26. Liu, X.; Wang, C.; Zhang, S.; Song, J.; Zhou, X.; Zha, M.; Wang, H. Fe-Bearing Phase Formation, Microstructure Evolution, and Mechanical Properties of Al-Mg-Si-Fe Alloy Fabricated by the Twin-Roll Casting Process. *J. Alloys Compd.* **2021**, *886*, 161202. [[CrossRef](#)]
27. Furu, M.; Kitamura, T.; Ishikawa, T.; Ikeno, S.; Saikawa, S.; Sakai, N. Evaluation of Age Hardening Behavior Using Composite Rule and Microstructure Observation in Al-Si-Mg Alloy Castings. *Mater. Trans.* **2011**, *52*, 1163–1167. [[CrossRef](#)]
28. Drouzy, M.; Jacob, S.; Richard, M. Interpretation of Tensile Results by Means of a Quality Index. *AFS Int. Cast Met. J.* **1980**, *5*, 43–50.
29. Taylor, J.A.; StJohn, D.H.; Barresi, J.; Couper, M.J. An Empirical Analysis of Trends in Mechanical Properties of T6 Heat Treated Al-Si-Mg Casting Alloys. *Int. J. Cast Met. Res.* **2000**, *12*, 419–430. [[CrossRef](#)]
30. Fortini, A.; Merlin, M.; Fabbri, E.; Pirletti, S.; Garagnani, G.L. On the Influence of Mn and Mg Additions on Tensile Properties, Microstructure and Quality Index of the A356 Aluminum Foundry Alloy. *Procedia Struct. Integr.* **2016**, *2*, 2238–2245. [[CrossRef](#)]
31. Ridgeway, C.D.; Gu, C.; Luo, A.A. Predicting Primary Dendrite Arm Spacing in Al-Si-Mg Alloys: Effect of Mg Alloying. *J. Mater. Sci.* **2019**, *54*, 9907–9920. [[CrossRef](#)]
32. Huang, C.; Liu, Z.; Li, J. Influence of Alloying Element Mg on Na and Sr Modifying Al-7Si Hypoeutectic Alloy. *Materials* **2022**, *15*, 1537. [[CrossRef](#)]
33. Stanić, D.; Brodarac, Z.Z.; Li, L. Influence of Copper Addition in AlSi7MgCu Alloy on Microstructure Development and Tensile Strength Improvement. *Metals* **2020**, *10*, 1623. [[CrossRef](#)]
34. Di Giovanni, M.T.; Mørtzell, E.A.; Saito, T.; Akhtar, S.; Di Sabatino, M.; Li, Y.; Cerri, E. Influence of Cu Addition on the Heat Treatment Response of A356 Foundry Alloy. *Mater. Today Commun.* **2019**, *19*, 342–348. [[CrossRef](#)]
35. Baskaran, J.; Raghuvaran, P.; Ashwin, S. Experimental Investigation on the Effect of Microstructure Modifiers and Heat Treatment Influence on A356 Alloy. *Mater. Today Proc.* **2021**, *37*, 3007–3010. [[CrossRef](#)]
36. Wang, E.R.; Hui, X.D.; Wang, S.S.; Zhao, Y.F.; Chen, G.L. Improved Mechanical Properties in Cast Al-Si Alloys by Combined Alloying of Fe and Cu. *Mater. Sci. Eng. A* **2010**, *527*, 7878–7884. [[CrossRef](#)]
37. Jeong, C. High Temperature Mechanical Properties of AlSiMg-(Cu) Alloys for Automotive Cylinder Heads. *Mater. Trans.* **2013**, *54*, 588–594. [[CrossRef](#)]

38. Bogdanoff, T.; Lattanzi, L.; Merlin, M.; Ghassemali, E.; Jarfors, A.E.W.; Seifeddine, S. The Complex Interaction between Microstructural Features and Crack Evolution during Cyclic Testing in Heat-Treated Al–Si–Mg–Cu Cast Alloys. *Mater. Sci. Eng. A* **2021**, *825*, 141930. [[CrossRef](#)]
39. Lumley, R.N.; Gunasegaram, D.R.; Gershenson, M.; O'Donnell, R.G. Effect of Alloying Elements on Heat Treatment Response of Aluminium High Pressure Die Castings. *Int. Heat Treat. Surf. Eng.* **2010**, *4*, 25–32. [[CrossRef](#)]
40. Yamamoto, K.; Takahashi, M.; Kamikubo, Y.; Sugiura, Y.; Iwasawa, S.; Nakata, T.; Kamado, S. Optimization of Cu Content for the Development of High-Performance T5-Treated Thixo-Cast Al–7Si–0.5Mg–Cu (Wt.%) Alloy. *J. Mater. Sci. Technol.* **2021**, *93*, 178–190. [[CrossRef](#)]
41. Ye, H. An Overview of the Development of Al-Si-Alloy Based Material for Engine Applications. *J. Mater. Eng. Perform.* **2003**, *12*, 288–297. [[CrossRef](#)]
42. Okayasu, M.; Sahara, N.; Mayama, N. Effect of the Microstructural Characteristics of Die-Cast ADC12 Alloy Controlled by Na and Cu on the Mechanical Properties of the Alloy. *Mater. Sci. Eng. A* **2022**, *831*, 142120. [[CrossRef](#)]
43. Zhang, W.; Ma, S.; Wei, Z.; Bai, P. The Relationship between Residual Amount of Sr and Morphology of Eutectic Si Phase in A356 Alloy. *Materials* **2019**, *12*, 3222. [[CrossRef](#)]
44. Nafisi, S.; Ghomashchi, R. Effects of Modification during Conventional and Semi-Solid Metal Processing of A356 Al-Si Alloy. *Mater. Sci. Eng. A* **2006**, *415*, 273–285. [[CrossRef](#)]
45. Vincze, F.; Tokár, M.; Fegyverneki, G.; Gyarmati, G. Examination of the Eutectic Modifying Effect of Sr on an Al-Si-Mg-Cu Alloy Using Various Technological Parameters. *Arch. Foundry Eng.* **2020**, *2020*, 79–84. [[CrossRef](#)]
46. Sigworth, G.K. The Modification of Al-Si Casting Alloys: Important Practical and Theoretical Aspects. *Int. J. Met.* **2008**, *2*, 19–40. [[CrossRef](#)]
47. Fracchia, E.; Gobber, F.S.; Rosso, M. Effect of Alloying Elements on the Sr Modification of Al-Si Cast Alloys. *Metals* **2021**, *11*, 342. [[CrossRef](#)]
48. Lee, P.D.; Sridhar, S. Direct Observation of the Effect of Strontium on Porosity Formation during the Solidification of Aluminium-Silicon Alloys. *Int. J. Cast Met. Res.* **2000**, *13*, 185–198. [[CrossRef](#)]
49. Miresmaeili, S.M.; Campbell, J.; Shabestari, S.G.; Boutorabi, S.M.A. Precipitation of Sr-Rich Intermetallic Particles and Their Influence on Pore Formation in Sr-Modified A356 Alloy. *Metall. Mater. Trans. A* **2005**, *36*, 2341–2349. [[CrossRef](#)]
50. Wang, Q.; Hao, Q.; Yu, W. Effect of Strontium Modification on Porosity Formation in A356 Alloy. *Int. J. Met.* **2019**, *13*, 944–952. [[CrossRef](#)]
51. Gyarmati, G.; Fegyverneki, G.; Tokár, M.; Mende, T. Investigation on Double Oxide Film Initiated Pore Formation in Aluminum Casting Alloys. *Int. J. Eng. Manag. Sci.* **2020**, *5*, 141–153. [[CrossRef](#)]
52. Flores, A.V.; Lopez, J.C.; Escobedo, J.C.B.; Castillejos, A.H.E.; Acosta, F.A.G. Effects of S and Sb Additions on the Microstructure and Mechanical Properties of the Al-Si 319 Alloy. *Can. Metall. Q.* **1994**, *33*, 133–138. [[CrossRef](#)]
53. Cai, Q.; Liu, B.; Chen, X.; Xi, W.; Cheng, J. Effect of Sb Modification and B Refinement on the Microstructure and Properties of As-Cast Al-7Si-0.35Mg Alloy. *Int. J. Met.* **2023**, *17*, 1065–1076. [[CrossRef](#)]
54. Jahromi, S.A.J.; Dehghan, A.; Malekjani, S. Effects of Optimum Amount of Sr and Sb Modifiers on Tensile, Impact and Fatigue Properties of A356 Aluminum Alloy. *Iran. J. Sci. Technol. Trans. B Eng.* **2004**, *28*, 225–232.
55. Fedak, M.; Rimar, M.; Corny, I.; Kuna, S. Experimental Study of Correlation of Mechanical Properties of Al-Si Casts Produced by Pressure Die Casting with Si/Fe/Mn Content and Their Mutual Mass Relations. *Adv. Mater. Sci. Eng.* **2013**, *2013*, 585514. [[CrossRef](#)]
56. Medlen, D.; Bolibruchova, D. Effect of Sb-Modification on the Microstructure and Mechanical Properties of Secondary Alloy 319. *Arch. Metall. Mater.* **2016**, *61*, 553–558. [[CrossRef](#)]
57. Pereira, C.L.; Gomes, L.F.; Garcia, A.; Spinelli, J.E. Comparing the Roles of Sb and Bi on Microstructures and Application Properties of the Al-15% Si Alloy. *J. Alloys Compd.* **2021**, *878*, 160343. [[CrossRef](#)]
58. Gursoy, O.; Timelli, G. The Role of Bismuth as Trace Element on the Solidification Path and Microstructure of Na-modified AlSi7Mg Alloys. *Adv. Eng. Mater.* **2023**, *25*, 2201377. [[CrossRef](#)]
59. Xu, C.; Xiao, W.; Hanada, S.; Yamagata, H.; Ma, C. The Effect of Scandium Addition on Microstructure and Mechanical Properties of Al-Si-Mg Alloy: A Multi-Refinement Modifier. *Mater. Charact.* **2015**, *110*, 160–169. [[CrossRef](#)]
60. Ma, Y.; Wang, M.; Liu, Y.; Cai, B. Microstructures and Corrosion Behaviors of Al–6.5Si–0.45Mg–XSc Casting Alloy. *Trans. Nonferrous Met. Soc. China* **2022**, *32*, 424–435. [[CrossRef](#)]
61. Pramod, S.L.; Ravikiran, Rao, A.K.P.; Murty, B.S.; Bakshi, S.R. Effect of Sc Addition and T6 Aging Treatment on the Microstructure Modification and Mechanical Properties of A356 Alloy. *Mater. Sci. Eng. A* **2016**, *674*, 438–450. [[CrossRef](#)]
62. Wang, M.; Guo, Y.; Wang, H.; Zhao, S. Characterization of Refining the Morphology of Al–Fe–Si in A380 Aluminum Alloy Due to Ca Addition. *Processes* **2022**, *10*, 672. [[CrossRef](#)]
63. Alkahtani, S. Effect of Mg, Sr, Ti and Aging Parameters on the Mechanical Behavior of 319 Alloys in the T5 and T6 Heat Treatment. *Adv. Mater. Res.* **2012**, *482–484*, 2275–2288. [[CrossRef](#)]
64. Tsai, Y.C.; Chou, C.Y.; Lee, S.L.; Lin, C.K.; Lin, J.C.; Lim, S.W. Effect of Trace La Addition on the Microstructures and Mechanical Properties of A356 (Al-7Si-0.35Mg) Aluminum Alloys. *J. Alloys Compd.* **2009**, *487*, 157–162. [[CrossRef](#)]

65. Nikitin, K.V.; Nikitin, V.I.; Deev, V.B. Effect of Adding Rare-Earth and Alkaline-Earth Metals to Aluminum-Based Master Alloys on the Structure and Properties of Hypoeutectic Siluminines. *Metallurgist* **2021**, *65*, 81–86. [[CrossRef](#)]
66. Totten, G.E.; Tiryakioglu, M.; Kessler, O. (Eds.) *Encyclopedia of Aluminum and Its Alloys*; CRC Press: Boca Raton, FL, USA, 2019.
67. Fan, Z.; Wang, Y.; Zhang, Y.; Qin, T.; Zhou, X.R.; Thompson, G.E.; Pennycook, T.; Hashimoto, T. Grain Refining Mechanism in the Al/Al-Ti-B System. *Acta Mater.* **2015**, *84*, 292–304. [[CrossRef](#)]
68. Jia, Y.; Song, D.; Zhou, N.; Zheng, K.; Fu, Y.; Shu, D. In Situ Investigation of Si-poisoning Effect in Al–Cu–Si Alloys Inoculated by Al–5Ti–1B. *Acta Metall. Sin.* **2022**, *35*, 146–156. [[CrossRef](#)]
69. Azimi, H.; Nourouzi, S.; Jamaati, R. Effects of Ti Particles and T6 Heat Treatment on the Microstructure and Mechanical Properties of A356 Alloy Fabricated by Compcasting. *Mater. Sci. Eng. A* **2021**, *818*, 141443. [[CrossRef](#)]
70. Saheb, N.; Laoui, T.; Daud, A.R.; Harun, M.; Radiman, S.; Yahaya, R. Influence of Ti Addition on Wear Properties of Al-Si Eutectic Alloys. *Wear* **2001**, *249*, 656–662. [[CrossRef](#)]
71. Polkowska, A.; Boyko, V.; Czekaj, E.; Mikhalenkov, K.; Saja, K. Microstructural Evolution of an Al–Mg–Si–Mn–Fe Alloy Due to Ti and P Addition. *Int. J. Mater. Res.* **2021**, *112*, 695–705. [[CrossRef](#)]
72. Samuel, A.M.; Samuel, E.; Songmene, V.; Samuel, F.H. A Comparative Study of Grain Refining of Al-(7–17%) Si Cast Alloys Using Al-10% Ti and Al-4% B Master Alloys. *Materials* **2023**, *16*, 2867. [[CrossRef](#)]
73. Lee, C. Effect of Ti-B Addition on the Variation of Microporosity and Tensile Properties of A356 Aluminium Alloys. *Mater. Sci. Eng. A* **2016**, *668*, 152–159. [[CrossRef](#)]
74. Choudhary, C.; Sahoo, K.L.; Roy, H.; Mandal, D. Effect of Grain Refiner on Microstructural Feature Influence Hardness and Tensile Properties of Al-7Si Alloy. *J. Mater. Eng. Perform.* **2022**, *31*, 3262–3273. [[CrossRef](#)]
75. Wu, D.; Ma, S.; Jing, T.; Wang, Y.; Wang, L.; Kang, J.; Wang, Q.; Wang, W.; Li, T.; Su, R. Revealing the Mechanism of Grain Refinement and Anti Si-Poisoning Induced by (Nb, Ti)B<sub>2</sub> with a Sandwich-like Structure. *Acta Mater.* **2021**, *219*, 117265. [[CrossRef](#)]
76. Mao, G.; Tong, G.; Gao, W.; Liu, S.; Zhong, L. The Poisoning Effect of Sc or Zr in Grain Refinement of Al-Si-Mg Alloy with Al-Ti-B. *Mater. Lett.* **2021**, *302*, 130428. [[CrossRef](#)]
77. Huang, J.; Feng, L.; Li, C.; Huang, C.; Li, J.; Friedrich, B. Mechanism of Sc Poisoning of Al-5Ti-1B Grain Refiner. *Scr. Mater.* **2020**, *180*, 88–92. [[CrossRef](#)]
78. Gyarmati, G.; Fegyverneki, G.; Kéri, Z.; Molnár, D.; Tokár, M.; Varga, L.; Mende, T. Controlled Precipitation of Intermetallic (Al,Si)<sub>3</sub>Ti Compound Particles on Double Oxide Films in Liquid Aluminum Alloys. *Mater. Charact.* **2021**, *181*, 111467. [[CrossRef](#)]
79. Gyarmati, G.; Bubonyi, T.; Fegyverneki, G.; Tokár, M.; Mende, T. Interactions of Primary Intermetallic Compound Particles and Double Oxide Films in Liquid Aluminum Alloys. *Intermetallics* **2022**, *149*, 107681. [[CrossRef](#)]
80. Gurtaran, M.; Uludağ, M. Effect of Ti Addition Holding Time on Casting Quality and Mechanical Properties of A356 Alloy. *SN Appl. Sci.* **2020**, *2*, 1833. [[CrossRef](#)]
81. Li, P.; Liu, S.; Zhang, L.; Liu, X. Grain Refinement of A356 Alloy by Al-Ti-B-C Master Alloy and Its Effect on Mechanical Properties. *Mater. Des.* **2013**, *47*, 522–528. [[CrossRef](#)]
82. Li, D.; Yan, X.; Fan, Y.; Liu, G.; Nie, J.; Liu, X.; Liu, S. An Anti Si/Zr-Poisoning Strategy of Al Grain Refinement by the Evolving Effect of Doped Complex. *Acta Mater.* **2023**, *249*, 118812. [[CrossRef](#)]
83. Aryshenskii, E.; Lapshov, M.; Hirsch, J.; Kononov, S.; Bazhenov, V.; Drits, A.; Zaitsev, D. Influence of the Small Sc and Zr Additions on the As-Cast Microstructure of Al–Mg–Si Alloys with Excess Silicon. *Metals* **2021**, *11*, 1797. [[CrossRef](#)]
84. Zhang, M.; Wang, J.; Wang, B.; Xue, C.; Liu, X. Improving Mechanical Properties of Al–Si–Cu–Mg Alloys by Microalloying Sc Using Thermodynamic Calculations. *Calphad* **2022**, *76*, 102394. [[CrossRef](#)]
85. Wang, Z.; Liu, X.; Zhu, C.; Xue, J.; Guo, Z.; Zhang, Y.; Li, X. Influence of the Interaction between Si and Sc on the Microstructure and Tensile Properties of as Casted Al-Si-Sc Alloys. *J. Alloys Compd.* **2023**, *932*, 167650. [[CrossRef](#)]
86. Ramli, R.; Talari, M.K.; Arawi, A.Z.O. Microstructure and Mechanical Properties of Al-Si Cast Alloy Grain Refined with Ti-B-Sr-Sc-Mg. In Proceedings of the 2011 IEEE Colloquium on Humanities, Science and Engineering (CHUSER 2011), Penang, Malaysia, 5–6 December 2011; pp. 692–695.
87. Puparattanapong, K.; Pandee, P.; Boontein, S.; Limmaneevichitr, C. Fluidity and Hot Cracking Susceptibility of A356 Alloys with Sc Additions. *Trans. Indian Inst. Met.* **2018**, *71*, 1583–1593. [[CrossRef](#)]
88. Patakham, U.; Kajornchaiyakul, J.; Limmaneevichitr, C. Grain Refinement Mechanism in an Al-Si-Mg Alloy with Scandium. *J. Alloys Compd.* **2012**, *542*, 177–186. [[CrossRef](#)]
89. Ding, J.; Lu, C.; Sun, Y.; Cui, C.; Zhao, E. Refining and Modification Effects of (Al, Zr, Si)-Al<sub>4</sub>Sr on Al-7Si-0.5Mg Alloy. *J. Mater. Res. Technol.* **2021**, *15*, 1604–1612. [[CrossRef](#)]
90. Cui, X.L.; Wu, Y.Y.; Gao, T.; Liu, X.F. Preparation of a Novel Al-3B-5Sr Master Alloy and Its Modification and Refinement Performance on A356 Alloy. *J. Alloys Compd.* **2014**, *615*, 906–911. [[CrossRef](#)]
91. Apparao, K.C.; Bannaravuri, P.K.; Pulisheru, K.S.; Francis, E.D.; Sunny, K.A.; Rao, G.B.; Daniel, P.F.; Birru, A.K. Effect of Novel Grain Refiner and Ni Alloying Additions on Microstructure and Mechanical Properties of Al-Si 9.8-Cu 3.4 HPDC Castings—Optimization Using Multi Criteria Decision Making Approach. *Mater. Sci.* **2022**, *40*, 9–24. [[CrossRef](#)]
92. Xiao, F.; Wu, M.; Wang, Y.; Wang, S.; Shu, D.; Wang, D.; Zhu, G.; Mi, J.; Sun, B. Design of Newly Effective Grain Refiner for Aluminum Based on Medium-Entropy Metal Diboride. *Vacuum* **2022**, *205*, 111462. [[CrossRef](#)]
93. Li, R.; Feng, Y.; Fu, Y.; Zhao, S.; Wang, L.; Guo, E. Effect of Composite Refining Modifier on Microstructure and Properties of AlSi10Mg Alloy. *J. Mater. Eng. Perform.* **2022**, *32*. [[CrossRef](#)]



94. Narducci, C.; Antunes, A.S.; Abdalla, A.J. Effect of the Heterogeneous Nucleation of the Primary  $\alpha$ -Al Grain via the Al-4Nb-0.5B Master Alloy in Al-Si Alloys with High Fe Contents. *Mater. Res.* **2021**, *24*, e2020544. [[CrossRef](#)]
95. Nowak, M.; Bolzoni, L.; Hari Babu, N. Grain Refinement of Al-Si Alloys by Nb-B Inoculation. Part I: Concept Development and Effect on Binary Alloys. *Mater. Des.* **2015**, *66*, 366–375. [[CrossRef](#)]
96. Bolzoni, L.; Hari Babu, N. Refinement of the Grain Size of the LM25 Alloy (A356) by 96Al-2Nb-2B Master Alloy. *J. Mater. Process. Technol.* **2015**, *222*, 219–223. [[CrossRef](#)]
97. Bolzoni, L.; Nowak, M.; Hari Babu, N. Grain Refinement of Al-Si Alloys by Nb-B Inoculation. Part II: Application to Commercial Alloys. *Mater. Des.* **2015**, *66*, 376–383. [[CrossRef](#)]
98. Narducci, C.J.; Brollo, G.L.; Siqueira, R.H.M.; Antunes, A.S.; Abdalla, A.J. Effect of Nb Addition on the Size and Morphology of the  $\beta$ -Fe Precipitates in Recycled Al-Si Alloys. *Sci. Rep.* **2021**, *11*, 9613. [[CrossRef](#)]
99. Taylor, J.A. Iron-Containing Intermetallic Phases in Al-Si Based Casting Alloys. *Procedia Mater. Sci.* **2012**, *1*, 19–33. [[CrossRef](#)]
100. Shabestari, S.G.; Mahmudi, M.; Emamy, M.; Campbell, J. Effect of Mn and Sr on Intermetallics in Fe-Rich Eutectic Al-Si Alloy. *Int. J. Cast Met. Res.* **2002**, *15*, 17–24. [[CrossRef](#)]
101. Szymczak, T.; Gumienny, G.; Klimek, L.; Goły, M.; Szymczak, J.; Pacyniak, T. Characteristics of Al-Si Alloys with High Melting Point Elements for High Pressure Die Casting. *Materials* **2020**, *13*, 4861. [[CrossRef](#)] [[PubMed](#)]
102. Zhang, X.; Wang, D.; Nagaumi, H.; Zhou, Y.; Yu, W.; Chong, X.; Li, X.; Zhang, H. Morphology, Thermal Stability, Electronic Structure and Mechanical Properties of  $\alpha$ -AlFeMnSi Phases with Varying Mn/Fe Atomic Ratios: Experimental Studies and DFT Calculations. *J. Alloys Compd.* **2022**, *901*, 163523. [[CrossRef](#)]
103. Tian, N.; Wang, G.; Zhou, Y.; Liu, C.; Liu, K.; Zhao, G.; Zuo, L. Phase Formation and Microstructure Evolution of Al-5Si-0.8Mg Alloys with Different Mn Concentrations. *Metals* **2021**, *11*, 308. [[CrossRef](#)]
104. Zhang, L.; Gao, J.; Damoah, L.; Robertson, D.G. Removal of Iron from Aluminum: A Review. *Miner. Process. Extr. Metall. Rev.* **2012**, *33*, 99–157. [[CrossRef](#)]
105. Hwang, J.Y.; Doty, H.W.; Kaufman, M.J. The Effects of Mn Additions on the Microstructure and Mechanical Properties of Al-Si-Cu Casting Alloys. *Mater. Sci. Eng. A* **2008**, *488*, 496–504. [[CrossRef](#)]
106. Jeong, C.Y.; Kang, C.; Cho, J. Effect of Alloying Elements on Mechanical Properties for A356 Casting Alloy. *Adv. Mater. Res.* **2007**, *26–28*, 111–114. [[CrossRef](#)]
107. Kuchariková, L.; Medvecká, D.; Tillová, E.; Belan, J.; Kritikos, M.; Chalupová, M.; Uhrčík, M. The Effect of the  $\beta$ -Al<sub>5</sub>FeSi Phases on Microstructure, Mechanical and Fatigue Properties in A356.0 Cast Alloys with Higher Fe Content without Additional Alloying of Mn. *Materials* **2021**, *14*, 1943. [[CrossRef](#)]
108. Dinnis, C.M.; Taylor, J.A.; Dahle, A.K. Interactions between Iron, Manganese, and the Al-Si Eutectic in Hypoeutectic Al-Si Alloys. *Metall. Mater. Trans. A* **2006**, *37*, 3283–3291. [[CrossRef](#)]
109. Chen, H.L.; Chen, Q.; Du, Y.; Bratberg, J.; Engström, A. Update of Al-Fe-Si, Al-Mn-Si and Al-Fe-Mn-Si Thermodynamic Descriptions. *Trans. Nonferrous Met. Soc. China* **2014**, *24*, 2041–2053. [[CrossRef](#)]
110. Švecová, I.; Tillová, E.; Kuchariková, L.; Knap, V. Possibilities of Predicting Undesirable Iron Intermetallic Phases in Secondary Al-Alloys. *Transp. Res. Procedia* **2021**, *55*, 797–804. [[CrossRef](#)]
111. Dunn, R. Aluminum Melting Problems and Their Influence on Furnace Selection. *Die Cast. Eng. B* **1965**, *9*, 8–30.
112. Wang, B.; Wang, J.; Liu, X.; Li, Q.; Liu, X. Uncovering the Effects of Neutralizing Elements (Co, Mn and Cr) on the Fe-Rich Intermetallic Formation in Al-Si-Cu Alloys. *Mater. Sci. Eng. A* **2022**, *858*, 144090. [[CrossRef](#)]
113. Kim, H.Y.; Han, S.W.; Lee, H.M. The Influence of Mn and Cr on the Tensile Properties of A356-0.20Fe Alloy. *Mater. Lett.* **2006**, *60*, 1880–1883. [[CrossRef](#)]
114. Kumar, L.; Cheol, J.; Hui, J.; Kwang, S.S. Effects of Cr and Ti Addition on Mechanical Properties and Thermal Conductivity of Al-7Si-3Mg Die-casting Alloys. *Met. Mater. Int.* **2022**, *29*, 204–214. [[CrossRef](#)]
115. Liu, N.; Jiang, B.; Wang, Y.; Ji, Z.; Hu, M.; Xu, H. Influence of Trace Amount Chromium on Microstructure and Corrosion Behavior of A356-5vol.%TiB<sub>2</sub> Alloy. *Mater. Lett.* **2022**, *314*, 131798. [[CrossRef](#)]
116. Ling, H.; Shi, H.; Du, X.; Zan, J.; Liu, J. Effect of Chromium Content on Microstructure and Properties of Casting Al-7Si-0.35Mg-0.02Sr Alloy. *Materwiss. Werksttech.* **2022**, *53*, 1229–1241. [[CrossRef](#)]
117. Liang, Y.; Cui, C.; Geng, H.; Liu, L.; Zhang, S.; Jin, R. Synergistic Effects of Cr and Sr Addition on the Mechanical and Corrosion Properties of A356.2 Alloy. *Mater. Charact.* **2022**, *191*, 112152. [[CrossRef](#)]
118. Li, Y.; Yang, Y.; Wu, Y.; Wei, Z.; Liu, X. Supportive Strengthening Role of Cr-Rich Phase on Al-Si Multicomponent Piston Alloy at Elevated Temperature. *Mater. Sci. Eng. A* **2011**, *528*, 4427–4430. [[CrossRef](#)]
119. Wang, X.; Ma, P.; Meng, Z.; Zhang, S.; Liu, X.; Wang, C.; Wang, H. Effect of Trace Cr Alloying on Centerline Segregations in Sub-Rapid Solidified Al-Mg-Si (AA6061) Alloys Fabricated by Twin-Roll Casting. *Mater. Sci. Eng. A* **2021**, *825*, 141896. [[CrossRef](#)]
120. Ludwig, T.H.; Schaffer, P.L.; Arnberg, L. Influence of Vanadium on the Microstructure of A356 Foundry Alloy. In *Light Metals 2013*; Sadler, B., Ed.; The Minerals, Metals & Materials Society: Pittsburgh, PA, USA, 2016; pp. 1023–1028.
121. Lin, B.; Li, H.; Xu, R.; Xiao, H.; Zhang, W.; Li, S. Effects of Vanadium on Modification of Iron-Rich Intermetallics and Mechanical Properties in A356 Cast Alloys with 1.5 Wt.% Fe. *J. Mater. Eng. Perform.* **2019**, *28*, 475–484. [[CrossRef](#)]
122. Medved, J.; Kores, S.; Vončina, M. Development of Innovative Al-Si-Mn-Mg Alloys with High Mechanical Properties. In *Light Metals 2018*; Martin, O., Ed.; The Minerals, Metals & Materials Society: Pittsburgh, PA, USA, 2018; pp. 373–380.

123. Morri, A.; Ceschini, L.; Messieri, S.; Cerri, E.; Toschi, S. Mo Addition to the A354 (Al–Si–Cu–Mg) Casting Alloy: Effects on Microstructure and Mechanical Properties at Room and High Temperature. *Metals* **2018**, *8*, 393. [[CrossRef](#)]
124. El Sebaie, O.; Samuel, A.M.; Samuel, F.H.; Doty, H.W. The Effects of Mischmetal, Cooling Rate and Heat Treatment on the Hardness of A319.1, A356.2 and A413.1 Al–Si Casting Alloys. *Mater. Sci. Eng. A* **2008**, *486*, 241–252. [[CrossRef](#)]
125. Petrov, I.A.; Shlyaptseva, A.D. Effect of REE on the Solidification of Eutectic Silumin. *Russ. Metall.* **2022**, *2022*, 204–210. [[CrossRef](#)]
126. Tao, C.; Huang, H.; Yuan, X.; Yue, C.; Su, M.; Zuo, X. Effect of Y Element on Microstructure and Hot Tearing Sensitivity of As-Cast Al–4.4Cu–1.5Mg–0.15Zr Alloy. *Int. J. Met.* **2022**, *16*, 1010–1019. [[CrossRef](#)]
127. Cardinale, A.M.; Macciò, D.; Luciano, G.; Canepa, E.; Traverso, P. Thermal and Corrosion Behavior of as Cast Al–Si Alloys with Rare Earth Elements. *J. Alloys Compd.* **2017**, *695*, 2180–2189. [[CrossRef](#)]
128. Stroh, J.; Sediako, D.; Weiss, D. The Effect of Rare Earth Mischmetal on the High Temperature Tensile Properties of an A356 Aluminum Alloy. In *Light Metals 2021*; Perander, L., Ed.; The Minerals, Metals & Materials Society: Pittsburgh, PA, USA, 2021; pp. 184–191.
129. Zhu, M.; Jian, Z.; Yang, G.; Zhou, Y. Effects of T6 Heat Treatment on the Microstructure, Tensile Properties, and Fracture Behavior of the Modified A356 Alloys. *Mater. Des.* **2012**, *36*, 243–249. [[CrossRef](#)]
130. Ibrahim, M.F.; Abdelaziz, M.H.; Samuel, A.M.; Doty, H.W.; Samuel, F.H. Effect of Rare Earth Metals on the Mechanical Properties and Fractography of Al–Si-Based Alloys. *Int. J. Met.* **2020**, *14*, 108–124. [[CrossRef](#)]
131. Li, Y.; Wu, Y.; Qian, Z.; Liu, X. Effect of Co-Addition of RE, Fe and Mn on the Microstructure and Performance of A390 Alloy. *Mater. Sci. Eng. A* **2009**, *527*, 146–149. [[CrossRef](#)]
132. Heo, U.; Han, D.; Kim, S.; Mo, C.B. Microstructure, Mechanical, and Corrosion Properties of Al–10Si and Al–10Si–2Cu Alloys with Different La Contents. *Mater. Today Commun.* **2022**, *32*, 104005. [[CrossRef](#)]
133. Song, Z.; Li, D.; Liu, W.; Yang, H.; Cao, Y.; Bi, G. Effect of La and Sc Co-Addition on the Mechanical Properties and Thermal Conductivity of as-Cast Al–4.8% Cu Alloys. *Metals* **2021**, *11*, 1866. [[CrossRef](#)]
134. Wu, X.; Luo, W.; Zhang, H.; Zhang, H.; Jiang, H. Effect of La Addition on Microstructure and Mechanical Properties of Hypoeutectic Al–7Si Aluminum Alloy. *China Foundry* **2021**, *18*, 481–487. [[CrossRef](#)]
135. Zhang, X.; Yang, Y.; Jin, H.; Sui, Y.; Jiang, Y.; Wang, Q. Effect of Lanthanum Content on Microstructure and Mechanical Properties of Al–5Mg–2Si–0.6Mn Alloy in Squeeze Casting. *J. Mater. Res. Technol.* **2021**, *15*, 6025–6033. [[CrossRef](#)]
136. Wang, Y.; Liu, Q.; Yang, Z.; Qiu, C.; Tan, K. Effect of Ce Addition and Heat Treatment on Microstructure Evolution and Tensile Properties of Industrial A357 Cast Alloy. *Metals* **2020**, *10*, 1100. [[CrossRef](#)]
137. Qiu, M.; Du, X.; Zhang, Z.; Chen, C.; Lei, X. The Effects of Combined Addition of Ce and Yb on Microstructure and Mechanical Properties of Al–Si–Mg–Cu–Cr Casting Alloy. *J. Mater. Eng. Perform.* **2022**, *32*, 3443–3451. [[CrossRef](#)]
138. Mao, F.; Yan, G.; Xuan, Z.; Cao, Z.; Wang, T. Effect of Eu Addition on the Microstructures and Mechanical Properties of A356 Aluminum Alloys. *J. Alloys Compd.* **2015**, *650*, 896–906. [[CrossRef](#)]
139. Amer, S.M.; Glavatskikh, M.V.; Barkov, R.Y.; Khomutov, M.G.; Pozdniakov, A.V. Phase Composition and Mechanical Properties of Al–Si Based Alloys with Yb or Gd Addition. *Mater. Lett.* **2022**, *320*, 132320. [[CrossRef](#)]
140. Li, D.; Cui, C.; Wang, X.; Wang, Q.; Chen, C.; Liu, S. Microstructure Evolution and Enhanced Mechanical Properties of Eutectic Al–Si Die Cast Alloy by Combined Alloying Mg and La. *Mater. Des.* **2016**, *90*, 820–828. [[CrossRef](#)]
141. Qiu, C.; Miao, S.; Li, X.; Xia, X.; Ding, J.; Wang, Y.; Zhao, W. Synergistic Effect of Sr and La on the Microstructure and Mechanical Properties of A356.2 Alloy. *Mater. Des.* **2017**, *114*, 563–571. [[CrossRef](#)]
142. Wu, D.; Kang, J.; Feng, Z.; Su, R.; Liu, C.; Li, T.; Wang, L. Utilizing a Novel Modifier to Realize Multi-Refinement and Optimized Heat Treatment of A356 Alloy. *J. Alloys Compd.* **2019**, *791*, 628–640. [[CrossRef](#)]
143. Ding, W.; Gou, L.; Hu, L.; Zhang, H.; Zhao, W.; Ma, J.; Qiao, J.; Li, X. Modification of Eutectic Si in Hypoeutectic Al–Si Alloy with Novel Al–3Ti–4.35La Master Alloy. *J. Alloys Compd.* **2022**, *929*, 167350. [[CrossRef](#)]
144. Luo, Q.; Li, X.; Li, Q.; Yuan, L.; Peng, L.; Pan, F.; Ding, W. Achieving Grain Refinement of  $\alpha$ -Al and Si Modification Simultaneously by La–B–Sr Addition in Al–10Si Alloys. *J. Mater. Sci. Technol.* **2023**, *135*, 97–110. [[CrossRef](#)]
145. Alkahtani, S.A.; Elgallad, E.M.; Tash, M.M.; Samuel, A.M.; Samuel, F.H. Effect of Rare Earth Metals on the Microstructure of Al–Si Based Alloys. *Materials* **2016**, *9*, 45. [[CrossRef](#)] [[PubMed](#)]
146. Mahmoud, M.G.; Samuel, A.M.; Doty, H.W.; Valtierra, S.; Samuel, F.H. Effect of Solidification Rate and Rare Earth Metal Addition on the Microstructural Characteristics and Porosity Formation in A356 Alloy. *Adv. Mater. Sci. Eng.* **2017**, *2017*, 5086418. [[CrossRef](#)]
147. Wang, D.; Zhang, X.; Xu, S.; Nagaumi, H.; Li, X. Improvement of Mechanical Properties in Micro-Alloying Al–Si–Mg–Zn Cast Alloy. *Mater. Lett.* **2021**, *283*, 128810. [[CrossRef](#)]
148. Huang, H.; Hu, C.; Song, D.; Jia, Z.; Zhou, N. Microstructure Characteristics and Elevated-Temperature Tensile Properties of Al–7Si–0.3Mg Alloys with Zr and Hf Addition. *J. Mater. Eng. Perform.* **2021**, *30*, 9059–9066. [[CrossRef](#)]
149. Zamzu, C.O.; Mbuya, T.O.; Adenya, C.A.; Ngigi, T. Effect of Transition Elements Additions on Microstructure and Tensile Properties of a Secondary Al–7Si–Mg Cast Aluminum Alloy. *Int. J. Eng. Technol. Sci. Innov.* **2021**, *6*, 91–101. [[CrossRef](#)]
150. Hu, P.; Liu, K.; Pan, L.; Chen, X. Effects of Individual and Combined Additions of Transition Elements (Zr, Ti and V) on the Microstructure Stability and Elevated-Temperature Properties of Al–Cu 224 Cast Alloys. *Mater. Sci. Eng. A* **2023**, *867*, 144718. [[CrossRef](#)]
151. Li, D.; Liu, K.; Rakhmonov, J.; Chen, X. Enhanced Thermal Stability of Precipitates and Elevated-Temperature Properties via Microalloying with Transition Metals (Zr, V and Sc) in Al–Cu 224 Cast Alloys. *Mater. Sci. Eng. A* **2021**, *827*, 142090. [[CrossRef](#)]

152. Baradarani, B.; Raiszadeh, R. Precipitation Hardening of Cast Zr-Containing A356 Aluminium Alloy. *Mater. Des.* **2011**, *32*, 935–940. [[CrossRef](#)]
153. Kamińska, J.; Angrecki, M.; Dudek, P. The Effect of Zirconium as an Alloying Additive on the Microstructure and Properties of AlSi9Mg Alloy Cast in Sand Moulds. *Arch. Foundry Eng.* **2022**, *22*, 5–13. [[CrossRef](#)]
154. Huang, H.; Dong, Y.; Xing, Y.; Jia, Z.; Liu, Q. Low Cycle Fatigue Behaviour at 300 °C and Microstructure of Al-Si-Mg Casting Alloys with Zr and Hf Additions. *J. Alloys Compd.* **2018**, *765*, 1253–1262. [[CrossRef](#)]
155. Arriaga-Benitez, R.I.; Peguleryuz, M. The Synergistic Effects of Nano-Sized  $\alpha$ -Al(Mn,Cr,Fe)Si and Al-Si-Zr Dispersoids on the Creep Behavior Al-Si-Mg-Cu (Mn, Cr, Zr) Diesel Engine Alloy. *Mater. Sci. Eng. A* **2023**, *872*, 144949. [[CrossRef](#)]
156. Zhang, Z.; Arici, A.; Breton, F.; Chen, X. Influence of Transition Elements (Zr, V, and Mo) on Microstructure and Tensile Properties of AlSi8Mg Casting Alloys. *Can. Metall. Q.* **2023**. [[CrossRef](#)]
157. Gariboldi, E.; Confalonieri, C.; Colombo, M. High Temperature Behavior of Al-7Si-0.4Mg Alloy with Er and Zr Additions. *Metals* **2021**, *11*, 879. [[CrossRef](#)]
158. Colombo, M.; Albu, M.; Gariboldi, E.; Hofer, F. Microstructural Changes Induced by Er and Zr Additions to A356 Alloy Investigated by Thermal Analyses and STEM Observations. *Mater. Charact.* **2020**, *161*, 110117. [[CrossRef](#)]
159. Huang, H.; Li, W.; Hu, C.; Ding, L.; Jia, Z.; Zhou, N. Dispersoid Characteristics and Elevated Temperature Creep Resistance of Al-Si-Mg Cast Alloy with Zr Addition. *Mater. Sci. Eng. A* **2022**, *836*, 142570. [[CrossRef](#)]
160. Shi, Z.M.; Wang, Q.; Zhao, G.; Zhang, R.Y. Effects of Erbium Modification on the Microstructure and Mechanical Properties of A356 Aluminum Alloys. *Mater. Sci. Eng. A* **2015**, *626*, 102–107. [[CrossRef](#)]
161. Li, G.; Liao, H.; Zheng, J.; Chen, H.; Lu, L.; Yang, L. Micro-Alloying Effects of Mn and Zr on the Evolution of Ageing Precipitates and High Temperature Strength of Al-11.5Si-4Cu Alloy after a Long-Time Heat Exposure. *Mater. Sci. Eng. A* **2021**, *828*, 142121. [[CrossRef](#)]
162. Zhang, M.; Wang, J.; Wang, B.; Xue, C.; Liu, X. Quantifying the Effects of Sc and Ag on the Microstructure and Mechanical Properties of Al-Cu Alloys. *Mater. Sci. Eng. A* **2021**, *831*, 142355. [[CrossRef](#)]
163. Wei, Q.; Xu, H.; Bai, X.; Lian, P.; Wang, Y.; Mao, H.; Wang, C. Effect of Sc on Microstructure and Properties of A357 Alloy under Different Casting Conditions. *J. Mater. Res. Technol.* **2022**, *20*, 2051–2059. [[CrossRef](#)]
164. Li, G.; Liao, H.; Zheng, J.; Chen, H.; Qian, L.; Yang, M. Sc-Induced Great Increase in High Temperature Strength of Al-Si-Cu Heat-Resistant Alloy. *J. Alloys Compd.* **2022**, *925*, 166622. [[CrossRef](#)]
165. Pratheesh, K.; Ravi, M.; Kanjirathinkal, A.; Joseph, M.A. Effects of Sr and Pressure on Microstructure, Mechanical and Wear Properties of near Eutectic Al-Si Piston Alloys. *Int. J. Cast Met. Res.* **2015**, *28*, 301–309. [[CrossRef](#)]
166. Demirtaş, H.; Karakulak, E.; Babu, N.H. Understanding the Effect of Ni Content on Microstructure and Mechanical Properties of A384 HPDC Alloy. *J. Alloys Compd.* **2022**, *896*, 163111. [[CrossRef](#)]
167. Abdelaziz, M.H.; Elgallad, E.M.; Doty, H.W.; Samuel, F.H. Strengthening Precipitates and Mechanical Performance of Al-Si-Cu-Mg Cast Alloys Containing Transition Elements. *Mater. Sci. Eng. A* **2021**, *820*, 141497. [[CrossRef](#)]
168. Lattanzi, L.; Giovanni, M.T.; Giovagnoli, M.; Fortini, A.; Merlin, M.; Casari, D.; Di Sabatino, M.; Cerri, E.; Garagnani, G.L. Room Temperature Mechanical Properties of A356 Alloy with Ni Additions from 0.5 Wt to 2 Wt%. *Metals* **2018**, *8*, 224. [[CrossRef](#)]
169. Ozyurek, D.; Yildirim, M.; Yavuzer, B.; Simsek, I.; Tuncay, T. The Effect of Ni Addition on Microstructure and Mechanical Properties of Cast A356 Alloy Modified with Sr. *Met. Mater.* **2021**, *59*, 391–399. [[CrossRef](#)]
170. García-Hinojosa, J.A.; González, C.R.; González, G.M.; Houbaert, Y. Structure and Properties of Al-7Si-Ni and Al-7Si-Cu Cast Alloys Nonmodified and Modified with Sr. *J. Mater. Process. Technol.* **2003**, *143–144*, 306–310. [[CrossRef](#)]
171. Casari, D.; Ludwig, T.H.; Merlin, M.; Arnberg, L.; Garagnani, G.L. The Effect of Ni and V Trace Elements on the Mechanical Properties of A356 Aluminium Foundry Alloy in As-Cast and T6 Heat Treated Conditions. *Mater. Sci. Eng. A* **2014**, *610*, 414–426. [[CrossRef](#)]
172. Casari, D.; Ludwig, T.H.; Merlin, M.; Arnberg, L.; Garagnani, G.L. Impact Behavior of A356 Foundry Alloys in the Presence of Trace Elements Ni and V. *J. Mater. Eng. Perform.* **2015**, *24*, 894–908. [[CrossRef](#)]
173. Gursoy, O.; Colak, M.; Tur, K.; Dispinar, D. Characterization of Properties of Vanadium, Boron and Strontium Addition on HPDC of A360 Alloy. *Mater. Chem. Phys.* **2021**, *271*, 124931. [[CrossRef](#)]
174. Huang, J.; Zhou, X.; Guo, J.; Liao, H.; Du, J. Effect of Ni Addition on the Microstructure and Mechanical Properties of 6101 Aluminum Alloy with High Electrical Conductivity. *J. Mater. Eng. Perform.* **2022**, *31*, 8923–8931. [[CrossRef](#)]
175. Xavier, M.G.C.; Freitas, B.J.M.; Koga, G.Y.; Spinelli, J.E. Effects of Ni and Co on the Corrosion Resistance of Al-Si-Cu-Zn-Fe Alloys in NaCl Solution. *Metals* **2022**, *12*, 645. [[CrossRef](#)]
176. Wang, R.; Wang, D.; Nagaumi, H.; Wu, Z.; Zhang, X.; Li, X. Effect of Zn Content on Corrosion Resistance of As-Cast Al-6Si-3Cu Alloy. *Mater. Lett.* **2022**, *312*, 131658. [[CrossRef](#)]
177. Yongtao, X.; Zhifeng, Z.; Zhihua, G.; Yuelong, B.; Purui, Z.; Weimin, M. Effect of Main Elements (Zn, Mg and Cu) on the Microstructure, Castability and Mechanical Properties of 7xxx Series Aluminum Alloys with Zr and Sc. *Mater. Charact.* **2021**, *182*, 111559. [[CrossRef](#)]
178. Akopyan, T.K.; Belov, N.A.; Letyagin, N.V.; Milovich, F.O.; Lukyanchuk, A.A.; Fortuna, A.S. Influence of Indium Trace Addition on the Microstructure and Precipitation Hardening Response in Al-Si-Cu Casting Aluminum Alloy. *Mater. Sci. Eng. A* **2022**, *831*, 142329. [[CrossRef](#)]

179. Fang, N.; Zou, C.; Wei, Z.; Wang, H.; Zhang, R.; Ran, Z.; Chang, T. Microstructural Evolution and Mechanical Properties of Al-Si-Cu-(Ge)-(Mg) Alloy Solidified under High Pressure. *Mater. Sci. Eng. A* **2021**, *827*, 142065. [[CrossRef](#)]
180. Li, G.; Liao, H.; Teng, H.; Yang, L.; Guo, H. Refining Effect of Trace Addition of B and the Impurity Elements in Al-Si-Cu-Mn-Ni Heat-Resistant Alloy on Primary Mn-Rich Phase. *Mater. Lett.* **2021**, *311*, 131563. [[CrossRef](#)]

**Disclaimer/Publisher's Note:** The statements, opinions and data contained in all publications are solely those of the individual author(s) and contributor(s) and not of MDPI and/or the editor(s). MDPI and/or the editor(s) disclaim responsibility for any injury to people or property resulting from any ideas, methods, instructions or products referred to in the content.